1992

Sampling and anaylsis of trace metals in sediment interstitial waters

Russell Fairey
San Jose State University

Order Number 1348673

Sampling and analysis of trace metals in sediment interstitial waters

Fairey, Russell, M.S.

San Jose State University, 1992

U·M·I
300 N. Zeeb Rd.
Ann Arbor, MI 48106

SAMPLING AND ANALYSIS OF TRACE METALS IN SEDIMENT INTERSTITIAL WATERS

A Thesis

Presented to

The Faculty of Moss Landing Marine Laboratories

In Partial Fulfillment

of the Requirements for the Degree

Master of Sciences

in

Marine Sciences

By

Russell Fairey

May, 1992

Approved For Moss Landing Marine Laboratories

Kenneth S Johnson

Dr. Kenneth S. Johnson, Professor

Kenneth H. Coale

Dr. Kenneth H. Coale, Research Associate

William Broenkow

Dr. William W. Broenkow, Professor

Approved for The University

Serena M. Stanford

ABSTRACT

Sampling and Analysis of Trace Metals
In Sediment Interstitial Waters

by Russell Fairey

Fine scale sampling and analysis of pore waters, near the sediment-water interface, afford a unique perspective of the environmental and chemical conditions leading to the flux of dissolved trace metals from sediments and the diagenetic reactions that produce this flux. In this work, a whole core squeezing technique was developed and used to collect interstitial water samples at millimeter depth resolution near the sediment-water interface. Interstitial water samples were analyzed for trace metals, nutrients and dissolved organic carbon. Dissolved oxygen concentrations and pH were determined concurrently with electrodes placed in-line with sample effluent.

This technique was used to investigate trace metal cycling in sediments of two distinct marine environments: the oxygen minimum zone of the California continental margin and perturbed coastal sediments near a large southern California wastewater outfall. Trace metal flux calculations determined from pore water gradients provide data for new theories on trace metal cycling and early diagenesis in the near interface region of these environments.

ACKNOWLEDGEMENTS

To my mentors, Dr. Ken Johnson and Dr. Kenneth Coale, I would like to express my sincere thanks for the time, resources and guidance each has provided me. Their depth of knowledge and enthusiasm for their science, as well as life in general, have provided standards worthy of emulation.

Dr. William Broenkow has made me realize how much there is to learn, while still providing the inspiration to charge forward in this quest of knowledge.

Dr. Will Berelson should be recognized for his critical and valuable insight, as well as his sense of humor. He has shown me that science can be both rigorous and fun.

I wish to thank Ginger Elrod, Jocelyn Nowicki, Teresa Coley and Tammy Kilgore for their assistance in the analysis of samples, and for providing a laboratory environment in which it was always a pleasure to work.

I would like to acknowledge the educators, staff and students of Moss Landing Marine Laboratories for creating the personal environment so critical to my graduate education. A special thanks to Sue Yoder and the USC Sea Grant Program for their encouragement and financial support of my research. This work was also aided by a research grant from the National Science Foundation, NSF # OCE-8923057.

This thesis would not have been possible without the inspiration and constant encouragement from my best friend and wife, Ellen.

Preface

This thesis presents a new method for the study of dissolved trace metals in the interstitial waters of marine sediments. Chapter 1 is written as an introduction to the trace metal geochemistry of pore waters and outlines the current knowledge and sampling techniques in the field. The format of Chapters 2 and 3 reflect the style required by the scientific journals to which they are submitted for publication. Chapter 2, which will be submitted to Limnology and Oceanography, describes a new technique for the extraction of pore waters from sediments, with an emphasis on analyzing the samples for dissolved trace metals. This technique is used in an open ocean study along a transect across the California continental margin. Chapter 3, which is submitted to Environmental Science and Technology, presents a study of copper in the pore waters of coastal sediments near a large sewage outfall in southern California. The techniques described in Chapter 2 are used to estimate benthic metal fluxes from the sediments and comparisons are made with fluxes measured directly with a benthic flux chamber. The results are used to characterize the mobility and recycling of metals from sediments near the outfall. The thesis concludes (Chapter 4) with a discussion of the application of this technique to pore water and diagenetic studies. An Appendix is included to present the data from the following studies.

CONTENTS

LIST OF FIGURES

Figure Page

LIST OF TABLES

CHAPTER 1

Introduction

Recent advances in the development of analytical procedures and instrumentation, coupled with ultra-clean techniques for sampling and analysis, have given scientists the first reliable measurements of trace metal distributions from ocean waters (Bruland, 1983). With this knowledge though, comes the need to explain the patterns of these distributions through the physical, biological and chemical processes which occur in the marine environment. Sediments are one of the key arenas for these processes and provide the focus for a variety of current research projects.

Diagenesis has been defined by Berner (1980) as "the sum total of processes that bring about changes in sediments or sedimentary rocks subsequent to its deposition in water." The diagenetic environments in sediments can be differentiated by the types of oxidation and reduction reactions which occur during the decomposition of organic matter (Chester, 1991). Oxic environments are characterized by the presence of dissolved oxygen and utilization of organic carbon via aerobic metabolic pathways. Oxygen may penetrate to a depth of a meter in ocean sediments (Revsbech et al., 1980) or may be restricted to the top few millimeters (Reimers and Smith, 1986). Below this zone are anoxic environments with no measurable oxygen, where anaerobic metabolic pathways utilize secondary oxidants such as nitrate, manganese oxides, iron oxides and sulfate during the decomposition of organic matter

(Fig. 1). The vertical distributions of these zones are dependent upon the nature of the deposited organic matter and the rate at which the sediments accumulate. The chemical changes which occur in each of these zones, and at the boundaries between them, are a driving force in trace metal geochemistry. These changes can alter sediment minerals, the chemical composition of interstitial waters and the chemical composition of the overlying water column.

Interstitial water, or pore water, is sea water which is trapped in the spaces between sediment particles during particle deposition. The redox reactions discussed above take place in pore waters or on particle surfaces in contact with pore waters. Pore waters thus reflect both water column chemistry and sediment redox chemistry, with physical transport properties governing the exchanges between the two.

The studies presented here focus on pore waters and the processes which influence the transition metals, copper (Cu), manganese (Mn), cobalt (Co) and iron (Fe). These metals are of oceanographic interest due to their involvement in biological metabolic pathways and due to their accumulation in mineral phases and manganese nodules (Wong et al., 1983). The purposes of the following chapters are to describe the distribution of these dissolved metals in the interstitial waters of sediments and to present the possible geochemical mechanisms which lead to their mobility and cycling between

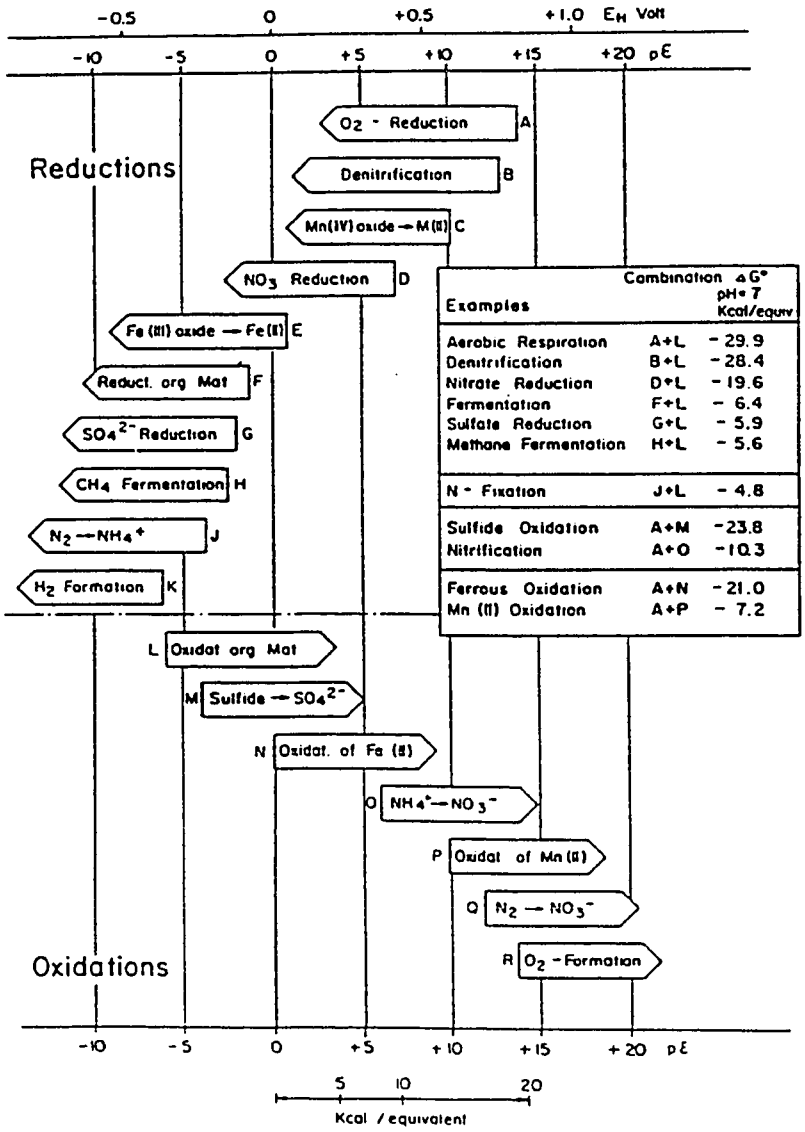

Figure 1) Diagenetic sequence of microbially mediated processes in sediments from Stumm and Morgan, 1981. sediments and the water column.

sediments and the water column.

There have been a number of previous studies of metal geochemistry in sediment pore waters, yet these studies have been limited by the resolution of the techniques which are available for the sampling of interstitial fluids. The sampling of sediments is accomplished by deploying instruments which physically grab surface sediments, or which penetrate the surface and retrieve a representative sediment core. Until recently, these instruments did not preserve the integrity of the overlying water and radically disturbed sediments near the sediment-water interface. This provided only a partial picture by effectively limiting pore water studies to the deeper (> 2 cm) diagenetic environments. Further complications were encountered during extraction of the interstitial water from sediments. Subsamples of sediment cores were sliced at 1-2 cm intervals and the sections centrifuged to separate pore waters from the solid phase (Sawlan and Murray, 1983; Heggie et al., 1986). Surface enrichments of some trace metals were consistently found in the top 1-2 cm sample interval (Fig. 2), yet the sampling resolution limited the definition of this observation. Suggestions by some researchers that trace metal redox zones may occur only millimeters below the sediment-water interface (Craven et al., 1986) mandated better sampling resolution in this region.

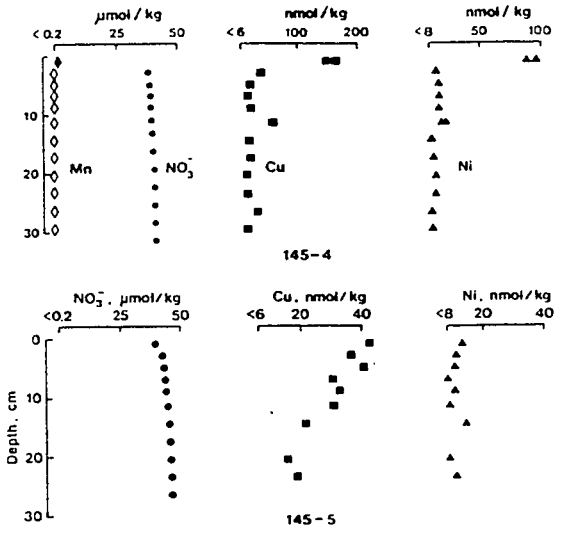

Figure 2a) Trace metal pore water profiles taken from Sawlan and Murray, 1983.

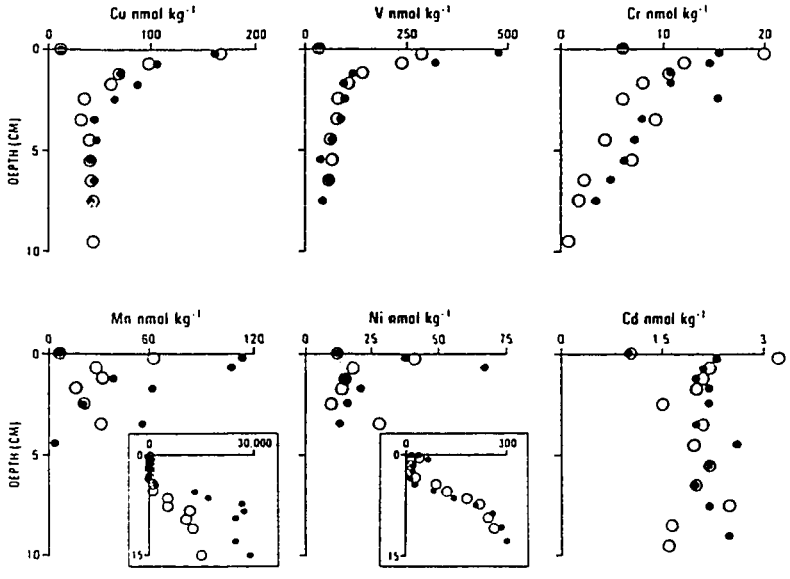

Figure 2b) Trace metal pore water profiles taken from Heggie, 1986.

Recent advances in the development of sediment boxcoring devices (Soutar et al., 1981; Heggie et al., 1986) have provided researchers with instruments which can sample the overlying water and superficial sediments with far less disturbance. This coupled with better resolution during subcore sectioning (0.25-0.5 cm) has resulted in enhanced sampling near the interface (Fig. 3) and yielded new insight to the early diagenesis of trace metals (Shaw et al., 1991).

The development of the whole core squeezing technique (Bender et al., 1987) is an recent advance in the extraction of pore waters. It provides an attractive alternative to sectioning since it is designed to sample pore waters at millimeter depth resolution, near the sediment-water interface. This is accomplished by mechanically applying pressure to pistons inside a tube containing a subcore sampled from the boxcore. The pressure moves the pistons together and forces pore waters from the interstitial spaces through a sampling port. This permits sampling of the bottom water overlying the subcore and of the interstitial waters at the sediment-water interface. The depth of each subsequent sample is calculated from the volume of water collected, the diameter of the subcore and the porosity of the sediment sample. The porosity of the sediment refers to the percentage of the sediment's total volume that is occupied by interstitial water. This method has been used successfully in determining

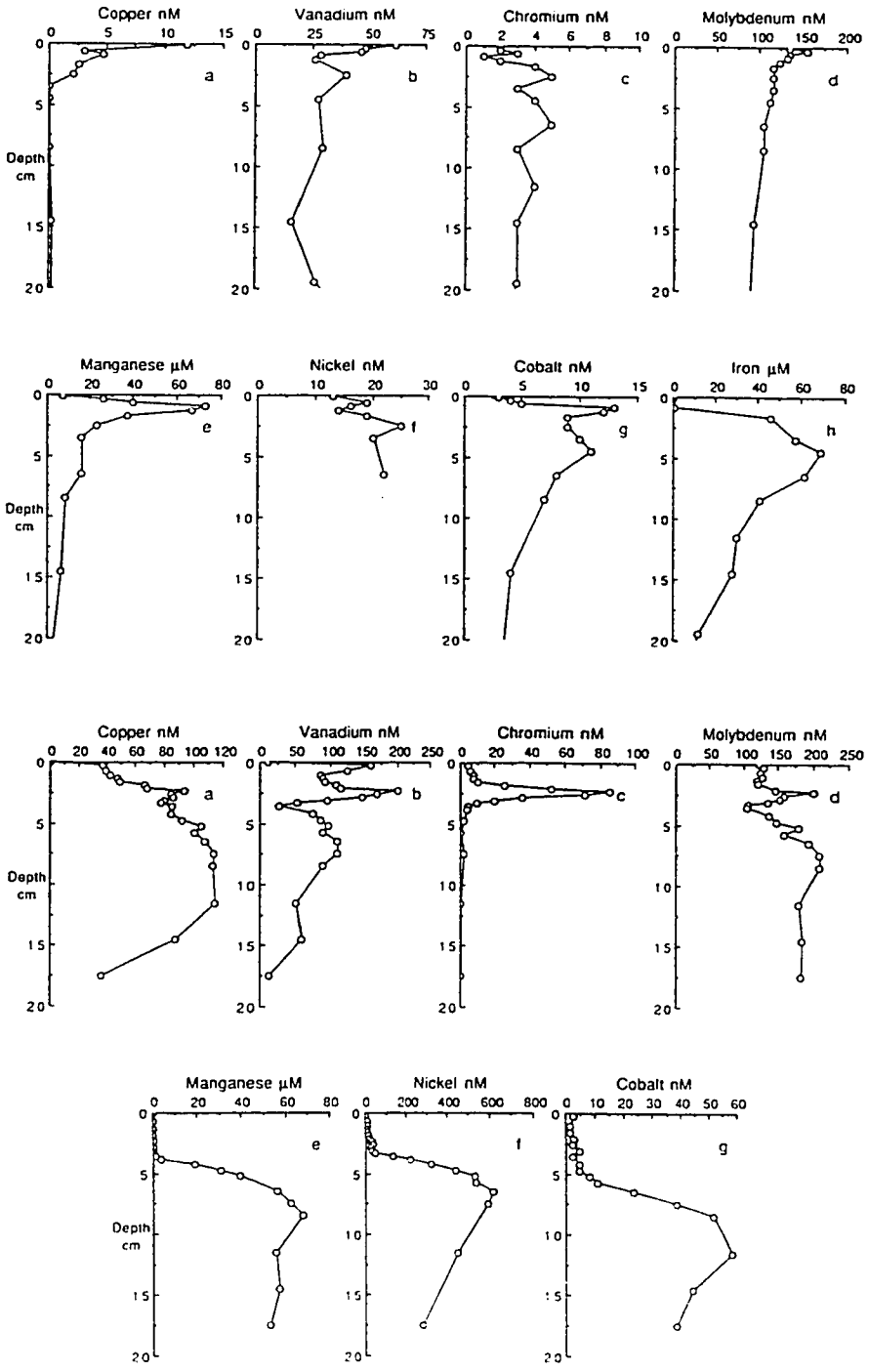

Figure 3) Pore water metal profiles taken from Shaw, 1990. The top panel is from the Santa Cruz Basin and the lower panel is from the Patton Escarpment.

the distribution of nutrients and other non-particle reactive ions in the interfacial region. This method has not been used, however, in determining trace metal distributions. The tendency of some trace metals to adsorb to particle surfaces has deterred the testing of this technique for its suitability in determining profiles of trace metals in pore waters. It was feared that these sorption properties could cause the smearing of chemical gradients as pore water flowed through the sediments during squeezing. Ongoing research in the field of metal-particle interactions has broadened our knowledge of the kinetics of these interactions though (Nyffeler et al., 1986; Honeyman and Santschi, 1988) and there are indications that some metal sorption rates may be sufficiently slow to be of minimal influence during squeezing (Jannasch et al., 1988).

Use of the whole core squeezing technique, for determining trace metals in superficial sediments, thus appears to be an approach worthy of examination. Adaptations are necessary to ensure that pore water samples are not contaminated with trace metals, as well as incorporation of sensors which will help identify the sedimentary redox conditions which are critical to understanding trace metal geochemistry. The development of this technique, coupled with improved boxcoring techniques, holds promise as a powerful tool in the study of trace metal diagenesis in sediments.

References

Bender, M., Martin, W., Hess, J., Sayles, F., Ball, L. and Lambert, C. (1987) A whole core squeezer for interfacial pore water sampling. Limnol. Oceanogr., **32**, 1214-1225

Berner, R.A. (1980) Early diagenesis: A Theoretical Approach. Princeton University Press, Princeton, N.J.

Bruland, K.W. (1983) Trace Elements in Sea-water. In: Chemical Oceanography, **8**, 157-220

Chester, R. (1990) Marine Geochemistry: Sediment interstitial water and diagenesis. Unwin Hyman Ltd., Winchester, Mass.

Craven, D.B., Jahnke, R. A. and Carlucci, A.F. (1986) Fine scale vertical distributions of microbial biomass and activity in California borderland sediments. Deep-Sea Res., **33**, 379-390

Heggie, D., Kahn, D. and Fisher, K. (1986) Trace metals in metalliferous sediments, MANOP Site M: interfacial pore water profiles. Earth and Planet. Sci. Lett., **80**, 106-116

Honeyman, B.D. and Santschi, P.H. (1988) Metals In Aquatic Systems. Environ. Sci. Technol., **22(8)**, 862-871

Jannasch, H.W., Honeyman, B.D., Balistrieri, L.S. and Murray, J.W. (1988) Kinetics of trace element uptake by marine particles. Geochim. Cosmochim. Acta, **(52)**, 567-577

Nyffeler, Y.P., Santschi, P.H. and Li, Y-H. (1986) The relevance of scavenging kinetics to modeling of sediment-water interactions in natural waters. Limnol. Oceanog., **31(2)**, 277-292

Reimers, C.E. and Smith, K.L., Jr. (1986) Reconciling measured and predicted fluxes of oxygen across the deep-sea sediment water interface. Limnol. Oceanogr., **31(2)**, 305-318

Revsbech, N.P., Jorgensen, B.B. and Blackburn, T.H. (1980) Oxygen in the sea bottom measured with a microelectrode. Science, **207**, 1355-1356

Sawlan, J.J. and Murray, J.W. (1983) Trace metal remobilization in the interstitial waters of red clay and hemipelagic marine sediments. Earth Planet. Sci. Lett., **64**, 213-230.

Shaw, T.J., Gieskes, J.W., and Jahnke, R.A. (1990) Early diagenesis in differing depositional environments: The response of transition metals in pore water. Geochim. Cosmochim. Acta, **54**, 1233-1246.

Soutar, A., Johnson, S., Fisher, K., and Dymond, J. (1981) Sampling the sediment-water interface for an organic rich surface layer. Trans. Am. Geophys. Union, **62**, 905

Stumm, W and Morgan, J.J. (1981) Aquatic Chemistry. New York: Wiley

Wong, C.S., Boyle, E., Bruland, K.W., Burton, J.D. and Goldberg, E.D. (eds) (1983) Trace Metals in Sea Water. Plenum Press, New York

CHAPTER 2

Trace Metal Analysis of Sediment Pore Waters: A Transect Through the Oxygen Minimum of the California Margin

Abstract

Fine scale sampling and analysis of pore waters near the sediment-water interface afford a unique perspective on the environmental and chemical conditions leading to the flux and diagenetic mobility of trace metals from sediments. Modified whole core squeezing techniques were used to collect interstitial water at the millimeter depth resolution. This technique was used to determine the distribution of metals near the sediment-water interface on a transect from the shelf through the oxygen minimum along the central California continental margin. Samples were analyzed for trace metals via flow injection analysis with chemiluminescence detection, as well as for nutrients and dissolved organic carbon. Concurrent pH and dissolved oxygen concentrations were determined with electrodes placed in-line with the sample effluent.

All metals exhibit sharp maxima just below the sediment-water interface in the 5-10 mm region. Metal maxima occur above the anoxic boundary and we observed a pH minimum associated with the iron(II) maximum. The metal maxima may be explained by the reduction of metal oxides, increased dissociation of organically bound metals during remineralization of organic matter or by non-steady state diagenesis due to the migration of redox fronts.

Trace metal flux calculations determined from pore water gradients indicate reduced flux from the oxygen minimum region. Observations suggest that oxic remineralization of organic carbon is the main factor controlling trace metal fluxes along the California continental margin.

Introduction

The processes leading to the exchange of heavy metals between ocean sediments and the overlying water column are still poorly understood, yet this knowledge is critical to further understanding the bio-geochemical cycling of trace metals in the world's oceans. Most previous pore water studies have addressed this problem with extraction techniques which physically limited the vertical sampling resolution in sediments to intervals $\geq$ 1 cm (Sawlan and Murray, 1983; Heggie et al., 1986). This usually involved slicing subcores into thin sections and centrifuging the sections for removal of pore water. The low sedimentation rates typical of those found in the open ocean made this type of sampling adequate for diagenetic studies over timescales on the order of 10,000 years. Lower rates of organic carbon consumption in these sediments spread the sequence of secondary oxidants (NO_3, MnO_2, Fe_2O_3 and SO_4) over a large depth range suitable for sampling by core sectioning techniques. Valuable data was gained on downcore metal concentrations (Klinkhammer, 1980), reaction sequences where oxidants were consumed in order of their decreasing free energies (Froelich et al., 1979) and on the distribution of oxidation fronts deep in sediments (Wilson et al., 1986). They also gave a picture of near surface (< 2 cm) enrichments of metals in the uppermost samples, yet gave

little insight to the mechanism of these enrichments.

Gradients in these pore water metal profiles were used to estimate benthic fluxes but the difficulty in distinguishing gradients near the sediment-water interface yielded large uncertainties in the modeling of the analytical results (Berelson and Hammond, 1986). Furthermore, the relatively high sedimentation and organic carbon consumption rates in coastal waters compress the diagenetic reaction sequence into the upper 1 cm of the sediments (Reimers, 1989). Shaw et al. (1990) addressed these problems by developing a method for sectioning a core with millimeter resolution. However, this method requires a refrigeration van, N_2 filled glove bag and cannot be used to sample O_2 or pH. There is thus a need for a simple pore water extraction technique which can sample the near interface region in order to determine trace metal profiles with sufficient resolution to accurately model benthic fluxes.

The whole core squeezing method, developed by Bender et al.(1987), utilizes mechanical force to squeeze pore water from interstitial spaces. It has been used for examination of nutrients and particle-unreactive ions in superficial sediments, with promising results. Tracer experiments and comparisons with other pore water extraction techniques agree favorably and support the validity of this method. However, the developers suggested caution in the use of this method for

determining profiles of dissolved particle reactive species such as trace metals. It was their fear that cation exchange on the solid phase of sediments could potentially introduce sampling artifacts as pore waters flowed through the core to the sample port during squeezing. This fear has been echoed by other pore water researchers (Sayles and Dickinson, 1991) yet no data has been presented to confirm or deny the hypothesis.

It was our belief that the whole core squeezing method could be modified to be useful in determining not only trace metal profiles but other important chemical characteristics of the sediments as well. In this way, superficial sediments can be examined with a focus on the conditions which determine trace metal mobility and cycling across the sediment-water interface. This study was thus initiated with two goals in mind: 1) To develop, low cost, whole core squeezing techniques for fine resolution analysis of trace metals in superficial sediments; and 2) To apply these techniques under a variety of open ocean conditions to examine the mechanisms of metal regeneration and cycling.

Instrument Description and Technique

The MLML whole core squeezer (WCS) was developed for laboratory or shipboard use in conjunction with standard

boxcoring techniques. It is most effective when used with coring devices which preserve the sediment-water interface and the overlying water, such as the Soutar type boxcores (Soutar, 1981). The MLML squeezer's major features consist of an aluminum support framework, 10 cm i.d. acrylic core tubes with sampling ports, a pressure regulated pneumatic ram with air supply valves, and pH and oxygen electrodes placed in-line with sample effluent. These features are shown in detail in Figure 1.

Subcore tubes are easily removed from the support framework by release of the coupler pin. Subcores may be taken by hand or by piston coring from the boxcore. For oxygen measurements, 5-10 cm of overlying water should be collected during subcoring. Upon return to the framework, the core tube is wrapped with a cooling jacket and maintained at bottom water temperature. Pressure is applied to the top piston by adjusting the air supply to the pneumatic ram. Initially an air pressure of $\approx$ 20 psi is sufficient to maintain a steady flow of sample effluent through the top piston and filters. Filter clogging and sediment compaction during the course of squeezing will slow effluent flow, so air pressure is slowly raised to compensate. Oxygen and pH electrodes are flow sensitive so maintaining a constant sample flow is critical for in-line measurements. This is easily accomplished with a fine adjustment pressure regulator on the

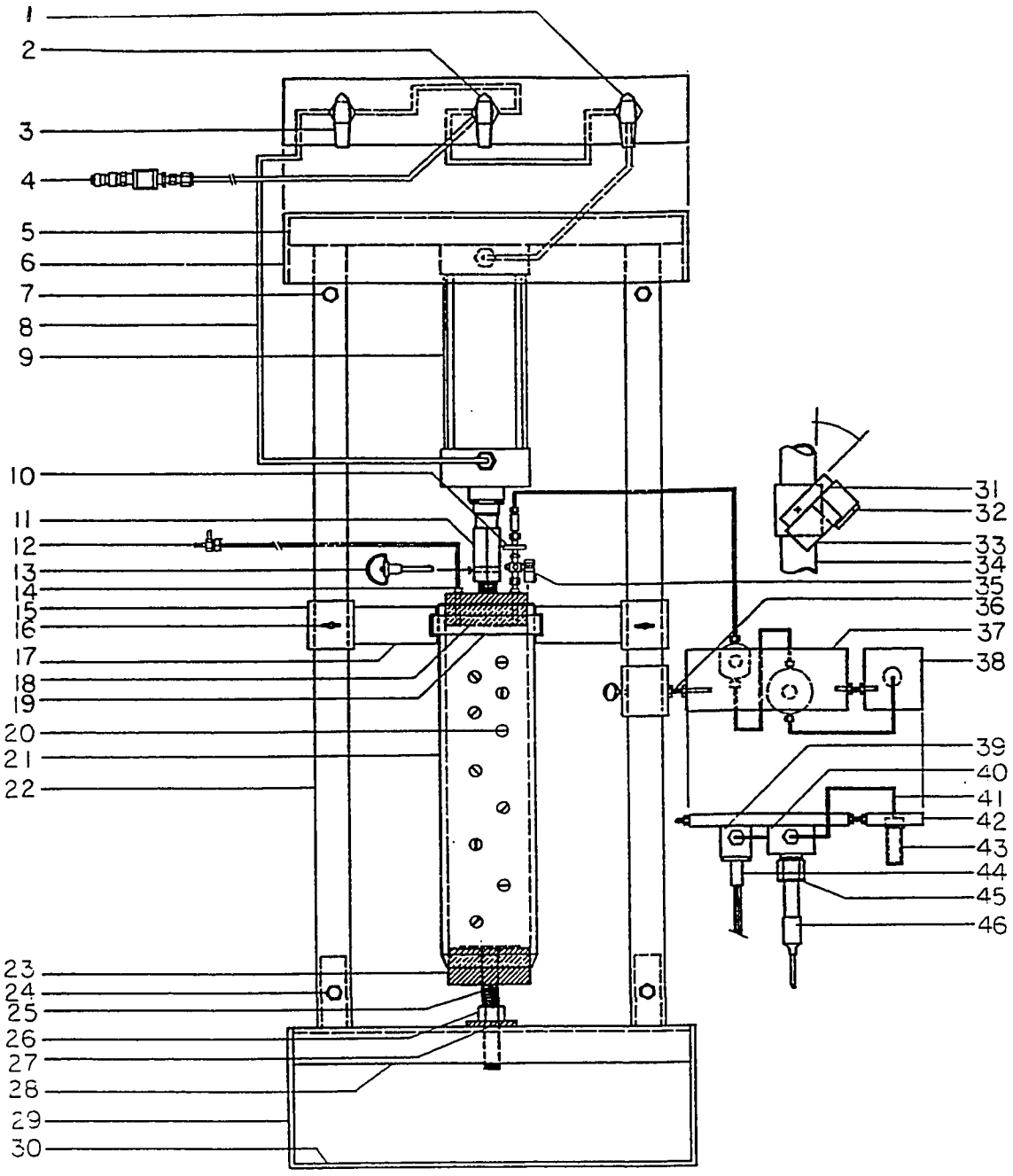

Figure 1) 1-3. Air Supply Valves (shown separated), 4. Pressure Regulator Adapter, 5. Pneumatic Ram Base, 6. Aluminum

Top Frame, 7. Support Tubing Pin, 8. Air Supply Line, 9. Bi-directional Pneumatic Ram, 10. 0.45μM Membrane Filter, 11. Ram/Piston Coupler, 12. Vent Valve and Line, 13. Coupler Pin, 14. Overlying Water Vent (1/4"-28 Leur-lock Connector), 15. Core Positioning Sleeve & Arm, 16. Wing Nuts, 17. Core Collar Locking Arm, 18. Top Piston with Channeling and Porous Polyethylene Pre-filter, 19. Acrylic Locking Collar, 20. 1/4-28 Side Sample Ports, 21. Acrylic Core Tube, 22. Support Tubing, 23. Bottom Piston, 24. Support Tubing Pin, 25. Piston Extension Bolt, 26. Piston Adjustment Nut, 27. Sleeve Washer, 28. 4" Aluminum Channel, 29. Bottom Frame Sides, 30. Bottom Frame Base, 31-34. Flow Cell Angle Adjustments to Eliminate Bubble Trapping (shown separated), 35. Top Sample Port Valve, 36. Angle Adjustment Bolt, 37-38. Acrylic Base Plates (Bottom View), 39. Oxygen Electrode Flow Cell, 40. pH Electrode Flow Cell, 41. Teflon Sample Line, 42. Acrylic Base Plate (Side View), 43. Teflon Sample Vial, 44. Oxygen Electrode, 45. Electrode/Flow Cell Coupler, 46. pH Electrode

air supply. The sensors are also sensitive to thermal changes so overlying water should be run for 5-10 minutes to stabilize the electrodes. Samples are extracted sequentially to a depth of $\approx$ 3 cm through the top piston while concurrent pH and oxygen measurements are recorded on a strip chart. Side ports are arranged for deeper sampling in the core, if desired.

Bubble trapping in filters, sample lines and electrode flow cells can be minimized by careful subcoring, line flushing with overlying water and proper angle positioning of flow cells.

Sampling and Analytical Procedures

The region selected for initial experiments was along the continental margin between Pt. Piedras Blancas and Pt. Sur,

off the central California coast (Fig 2). This area is characterized by a steep continental slope which reaches abyssal depths within 100km of shore, making it possible to sample a variety of sediment types and bottom depths with a minimum of ship time. An oxygen minimum zone impinges on the sediments of the slope and allows investigations to be made under a wide range of oxic conditions.

The oxygen minimum zone in this region is found between 500 m and 1000 m. Sediment samples from ten stations were obtained with a teflon coated 0.125 m^2 Soutar-type boxcore, at depths ranging from 99 m to 2006 m. Subcores were taken upon retrieval of the boxcore and transferred to the WCS. Squeezing was begun immediately to minimize any oxygen changes caused by respiration in the closed system. Overlying water is used to stabilize the electrodes, to purge the system and to determine if mixing of surface water occurred during boxcore retrieval. Mixing is suspect when subcore oxygen values are higher than determined for near bottom water with Niskin sampling and Winkler titrations. Filtered pore water samples (0.45 μm) were collected sequentially in approximately 7 ml aliquots. This volume corresponded with a piston displacement of approximately 1 mm in high porosity sediments.

To avoid trace metal contamination, all sample containers and WCS surfaces in contact with the sample were plastics (acrylic, PVC, TFE, PE and PP) and cleaned with Micro, 1N HCl

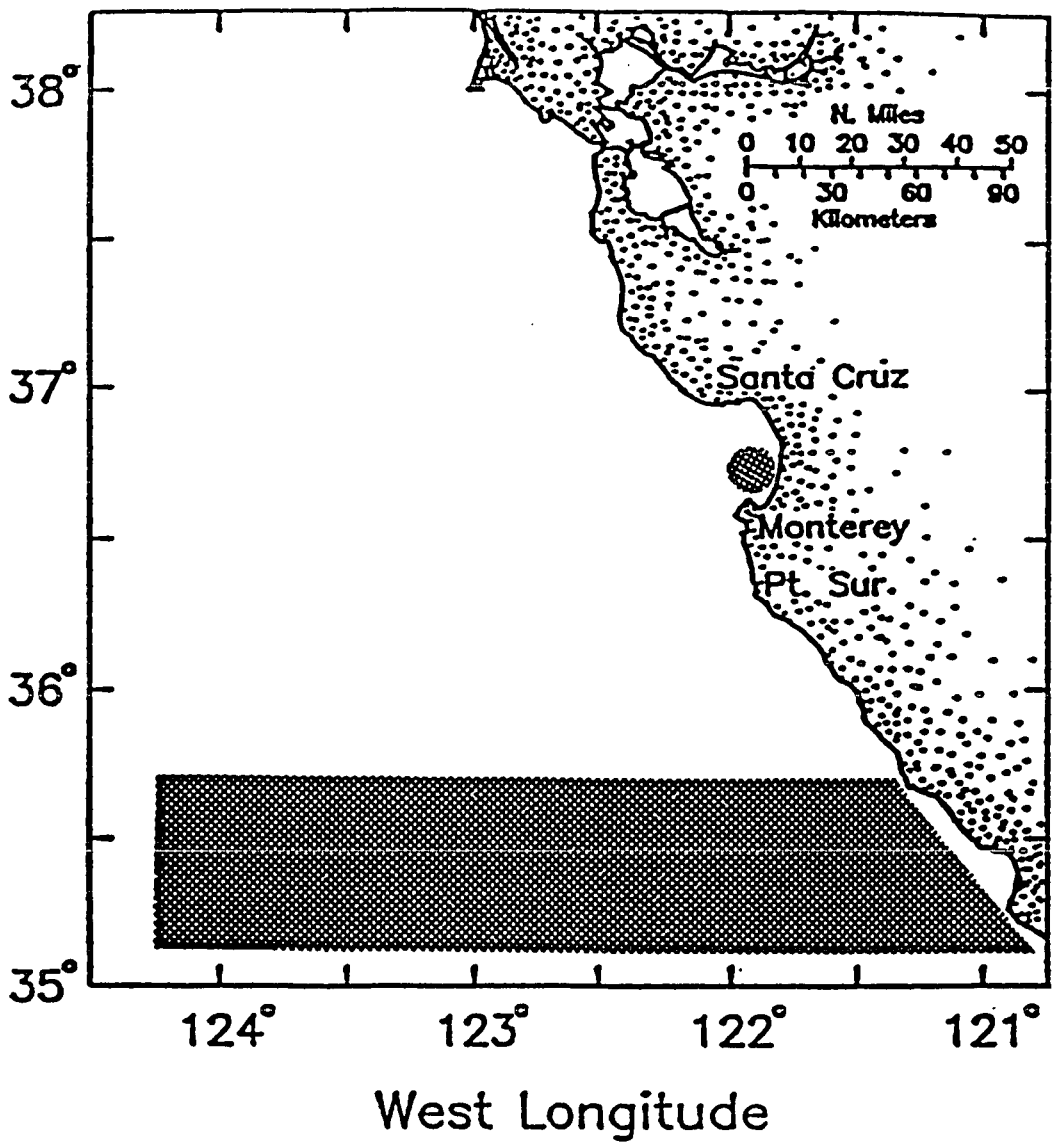

Figure 2) Study area from Teflon-1 cruise, June 5-28, 1991

and Millipore Milli-Q water. Subsamples were analyzed for nutrients using standard colorimetric techniques (Strickland and Parsons, 1972) and for the trace metals Co, Mn, Cu and Fe using flow injection analysis with chemiluminescence detection (Sakamoto-Arnold and Johnson, 1987; Chapin et al., 1991; Coale et al., in press; and Elrod et al., 1991). Prior to the FIA-CL analysis, subsamples were diluted (1+25) with purified Milipore Milli-Q water. Iron subsamples were acidified and analyzed immediately to minimize oxidation of Fe(II). Dissolved organic carbon subsamples were frozen for later laboratory analysis. Other subsamples were analyzed within 24 hours aboard ship.

Sediment solid phase samples were analyzed for porosity, organic carbon, and organic nitrogen. Porosity is expressed as per cent water, by volume, assuming a dry bulk density of 2.6 g/cm^3 and a porewater salinity of 35‰. Organic carbon and nitrogen in the solid phase were determined with a Perkin Elmer 440 Elemental Analyzer.

An additional experiment was performed to assess the feasibility of examining metal behavior by injecting dissolved metals into the core. Two subcores were collected from the 100 m station and the first squeezed normally. The second was "spiked" with a known concentration of the metals Cu, Mn and Co and with the non-particle reactive tracer CsCl prior to squeezing. The 250 μl spike was injected into the core, at a

depth of 3 cm below the sediment-water interface, with a 2 mm diameter needle. Pore water samples were analyzed for metals by graphite furnace atomic absorption and for CsCl by atomic emission spectroscopy.

Results and Discussion

A 25 minute portion of a typical core squeezing run is shown in the raw data of Figure 3, where sequential squeezer effluent samples are directly associated with continuous oxygen and pH readings. Time required to completely process a core in this manner is about two hours. Values for pH are reported in millivolts due to calibration difficulties encountered with changes in temperature over the bottom depth sampling range. Oxygen values (Fig. 4) are calculated from calibrations with air saturated water and deoxygenated water pumped through the system to mimic core squeezing. The results compare well with oxygen micro-electrode profiles of open ocean sediments from other studies (Reimers et al., 1986). A well defined minumum in pH is commonly found near the base of the oxic zone (Fig. 4). It is in this pH minimum region (< 1.5 cm) that changes in trace metal concentrations are most rapid and distinct metal maxima were found (Fig. 5).

To assess the extent of chromatographic effects the physical structure of the trace metal peaks and profiles were examined. If cationic sorption was limiting the flow of metals

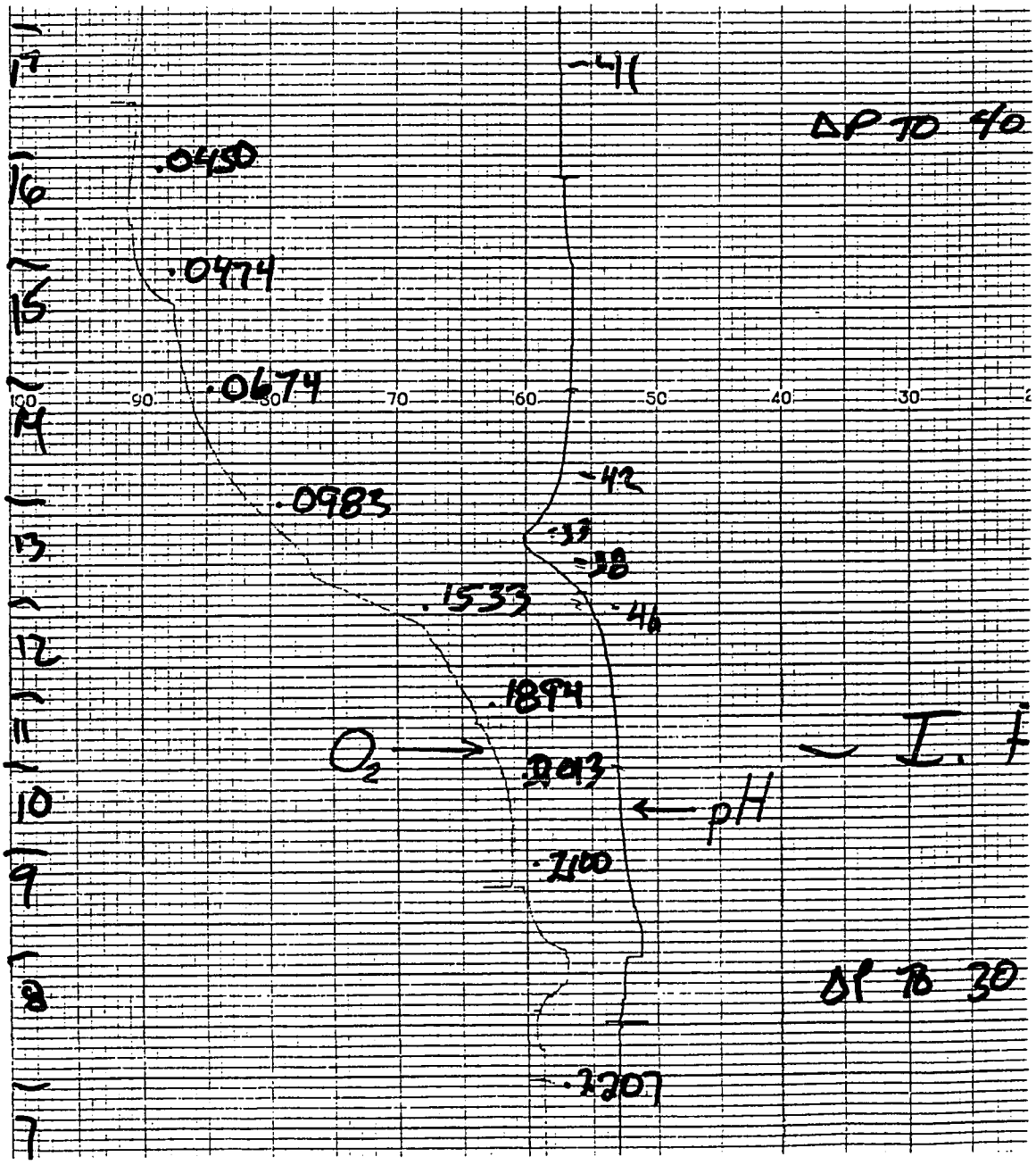

Figure 3) Strip chart recording of pore water pH (mvolts) and O_2 (volts) gradients. Sequential pore water samples are numbered and recorded for depth calculations. The sediment-water interface was at sample #7. Chart speed was 0.5 cm/min, so this represents approximately 25 minutes of a two hour squeezing run.

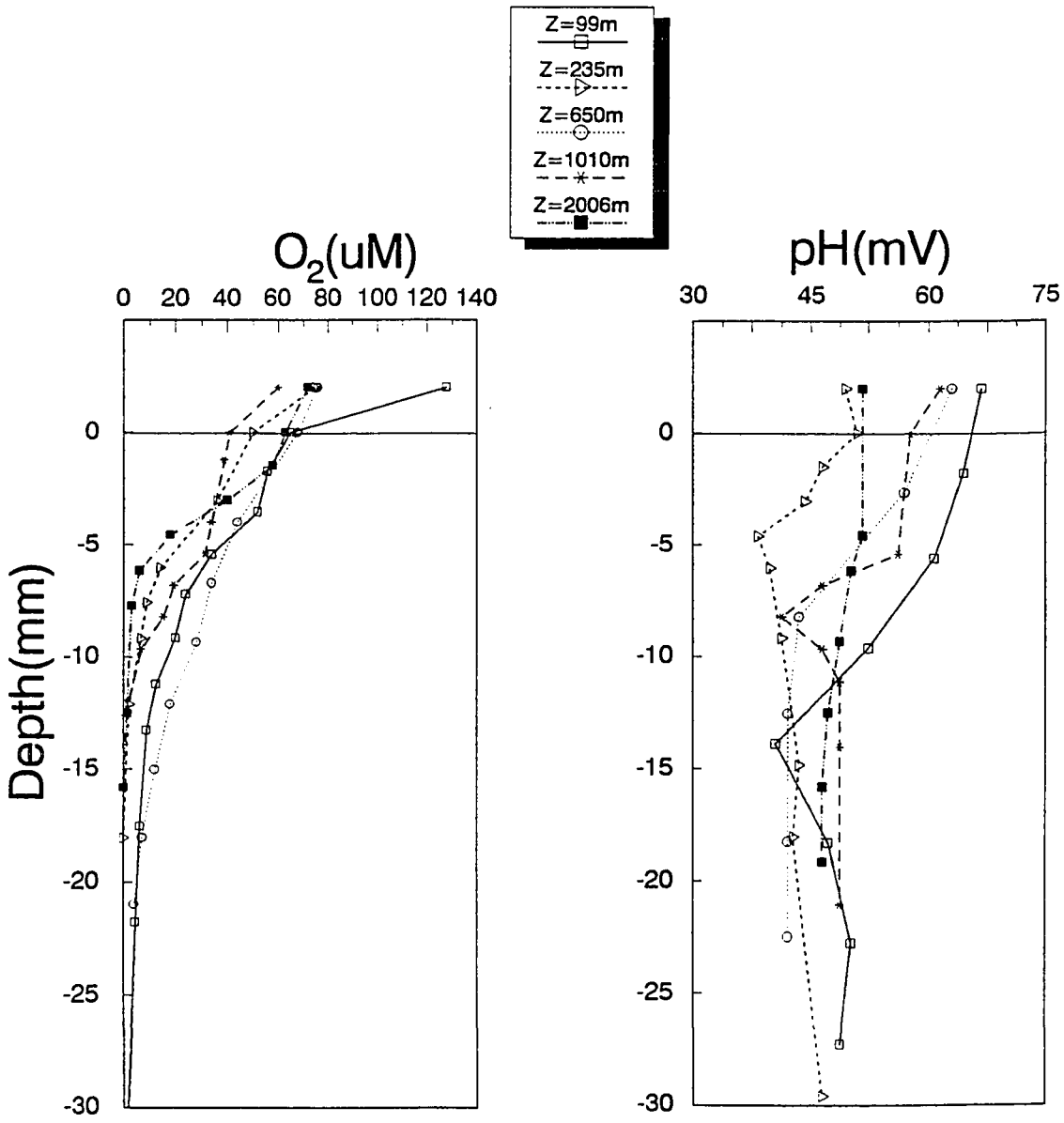

Figure 4) Oxygen and pH pore water profiles on a transect across the oxygen minimum. The high oxygen values shown at the 650m station were from a boxcore which was contaminated with surface water. Rapid identification of contaminated cores was useful in limiting unnecessary trace metal analysis.

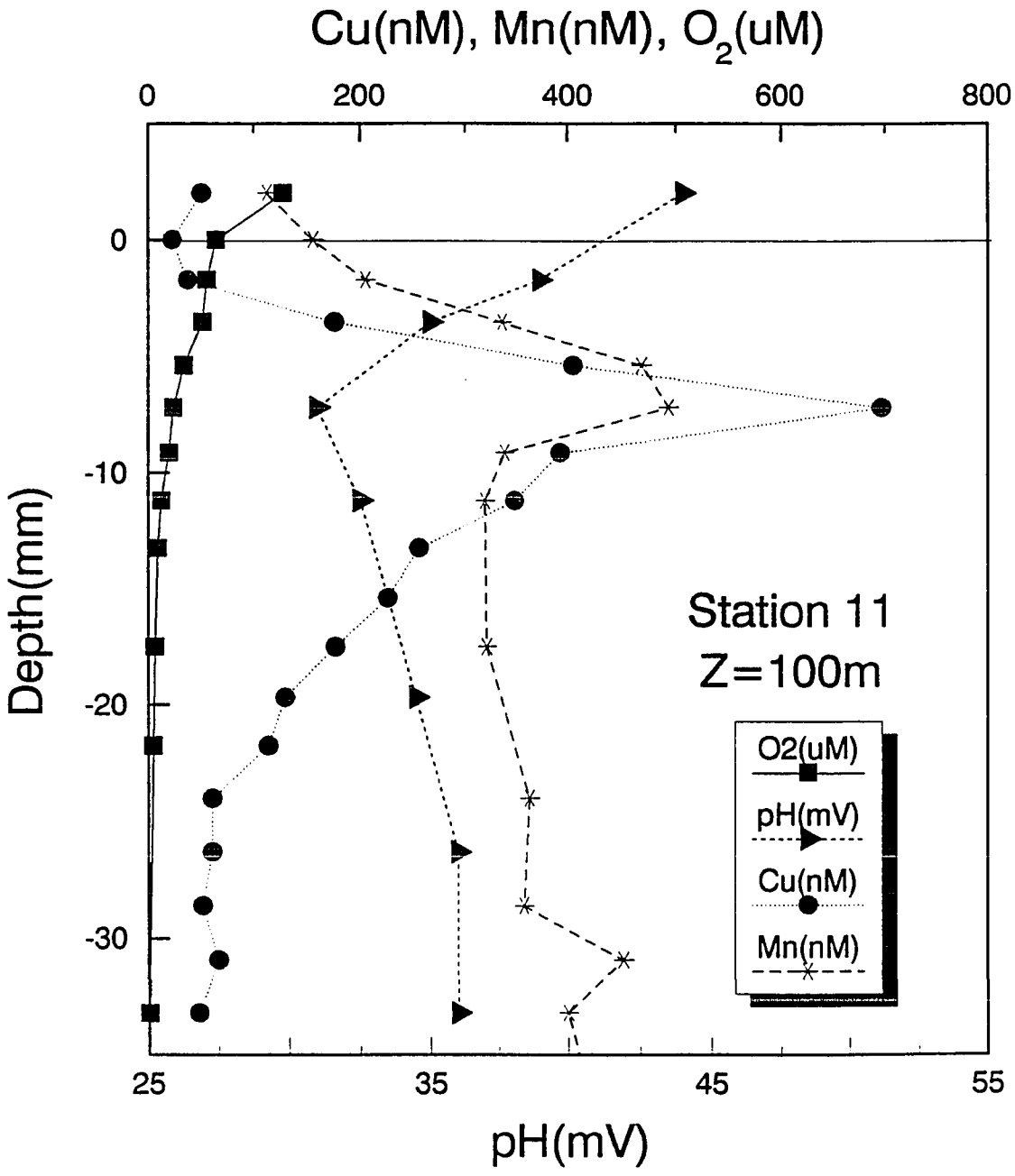

Figure 5) Pore water trace metal concentrations and redox conditions from a core retrieved from Monterey Bay.

through the sediment, two things should be expected. First, smearing effects would minimize and broaden metal peaks. The observed preservation of sharp metal maxima and steep gradients does not support this. An explanation for the missing chromatographic effects lies in recent laboratory sorption studies. Nyffeler et al. (1986) looked at the time dependence of trace element partitioning between natural waters and sediments. Time series measurements of the partition ratios K_d indicated that for some elements (Zn, Se, Cd, Sn, Ba, Th) K_d became constant after a few days of equilibration, while others (Fe, Mn, Co) showed time constants on the order of weeks. This is a major departure from earlier models which assumed instantaneous equilibrium adsorptions (Lerman, 1979 and Berner, 1980). It would indicate that scavenging kinetics in sediments are sufficiently slow to minimize any sampling artifacts created during any potential short term disequilibria encountered during squeezing. Second, each metal exhibits characteristic adsorption and binding kinetics (Honeyman and Santschi, 1988). It seems unlikely that surface complexation in sediments would affect all metal ion adsorption uniformly during the disequilibrium of squeezing. Therefore, if particle/metal reactions were significant, concurrent maxima for different metals would not be expected during the same sample interval.

This reasoning applies if metal maxima originally

coexisted at the same sediment depth. To attempt to create a known co-existence of metal peaks, a core was spiked with metals and a CsCl tracer. The 250 μl spike was injected at a depth of 3 cm below the interface, where in-situ metal concentrations were determined to be low during previous sampling. Comparison of pore water samples from the spiked and unspiked cores showed little change in trace metal or tracer concentration as a result of the spiking. It is theorized that the dissolved metals in the spike were precipitated as insoluble metal sulfides in this anoxic region of the core. This leaves a question as to the effectiveness of artificial spiking for evaluating dissolved metal behavior without also including solid phase metal analysis. Continued spiking research in this direction is recommended, as well as for near-interface oxic regions of the core for evaluation of metal-particle sorption properties.

Pore water trace metal concentrations from the continental shelf transect are shown in Figure 6. Maxima in the metal profiles are most prominent from sediments above and below the oxygen minimum zone. All metals exhibit their lowest subsurface concentrations at stations within the oxygen minimum.

So what produces this shallow subsurface trace metal maxima? A model to explain the metal maxima must account for the following observations. 1) The concentration maxima of the

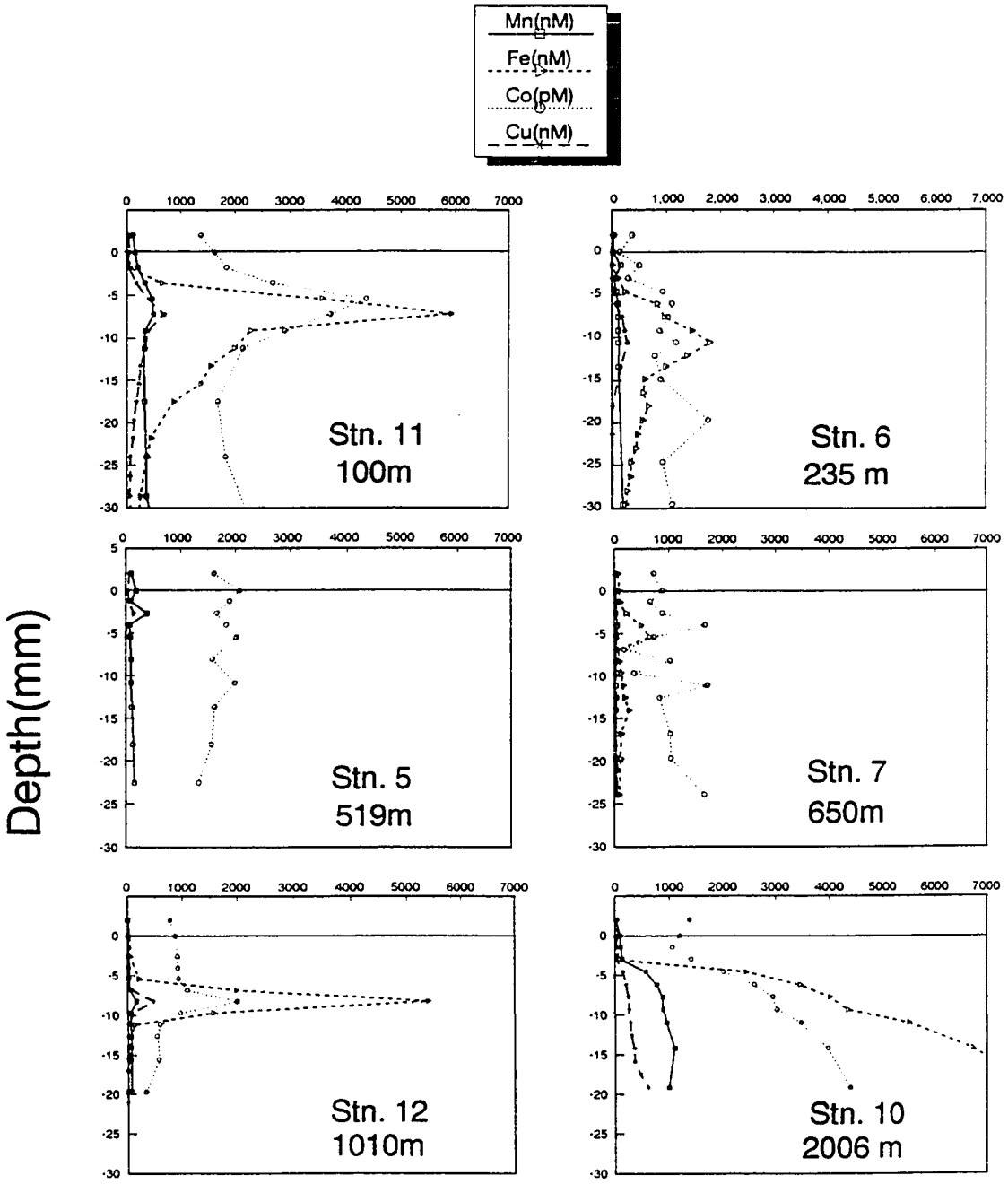

Figure 6) Pore water trace metal profiles for six stations on the California continental margin. The oxygen minimum region was located between 500 m and 1000 m.

four metals Cu, Mn, Co, and Fe are all coincident and yet these metals have considerable differences in geochemical properties. We must look to a process that can simultaneously release all metals. 2) The maxima occur within a pH minimum zone. The reaction releasing the metals must produce protons. 3) The reaction producing the metal maximums occurs as the oxygen concentration approaches zero. In contrast though, no metal maxima are found at the two stations within the core of the oxygen minimum zone where the lowest water column O_2 values are found. With these considerations in mind, we can examine the diagenetic reactions which affect dissolved metal concentrations in sediment pore waters.

Reduction of metal oxides deposited in oxic sediments will produce a large increase in dissolved Mn and Fe as the buried sediments go anoxic (Froelich et al., 1979). Other metals bound to the oxide phase may be released as well. However, in anaerobic metabolic pathways, the reduction of metals consumes protons and should produce a rise in pH.

$$(CH_2O)_{106}(NH_3)_{16}(H_3PO_4) + 236\ MnO_2 + 472\ H^+ \rightarrow$$
$$236\ Mn^{2+} + 106\ CO_2 + 8\ N_2 + H_3PO_4 + 366\ H_2O$$

$$(CH_2O)_{106}(NH_3)_{16}(H_3PO_4) + 212\ Fe_2O_3 + 848\ H^+ \rightarrow$$
$$424\ Fe^{2+} + 106\ CO_2 + 16\ NH_3 + H_3PO_4 + 530\ H_2O$$

We observe a sharp drop in pH in association with the metal maxima. Oxidation of reduced compounds, which have diffused

into the oxic interfacial region, could create this pH drop. These reduced compounds could be metals (Fe^{2+}, Mn^{2+}) or sulfide (HS^-).

$$4Fe^{2+} + O_2 + 6H_2O \rightarrow 4\ FeOOH + 8\ H^+$$

$$2\ Mn^{2+} + O_2 + 4H_2O \rightarrow 2MnO_2 + 4\ H^+$$

$$HS^- + 2\ O_2 \rightarrow SO_4^{2-} + H^+$$

A flux of metals from deeper in the sediment should not produce a concentration maximum, however. The metal maximum might be better explained by the following mechanism. Dissolved metals could be precipitated as insoluble metal sulfide minerals (Emerson, 1983) in the anoxic region below the metal maxima, thus driving down the dissolved metal concentration. The high dissolved concentrations nearer the interface would result from reduction of metal oxides as mentioned above. A net pH decrease would occur if HS^- oxidation outweighed oxide reduction.

Another possible explanation for the pH drop associated with the metal maxima relates to the oxidation of detrital organic matter. Release of organically bound metal ions during microbial degradation could result in rapid oxidation of the dissolved metals. Protons generated during the oxidation step could drive the pH drop and steep metal gradients associated with the metal maxima. These pH changes may further enhance release of other metals by shifting pH sensitive sorption equilibria (Honeyman and Santschi, 1988).

These explanations will be complicated if the diagenetic processes are not at a steady state in the sediments. It has been observed that migrating oxidation fronts can confuse the interpretation of trace metals in pore water data (Wilson et al., 1986 and Shaw et al., 1990). For example, seasonal or event-linked vertical migration of the oxic-anoxic interface may produce non-steady state enrichments from reduction and re-oxidation of upward diffusing iron oxides or iron sulfides. This effect may be particularly important in shallow sediments although we did observe a clear uniformity over the entire sampling transect, except in the core of the oxygen minimum.

Pore water gradients, in the enriched layers where maxima are found, were used to calculate flux values(J_s) for metals and nutrients at each station (Table 1), using Berner's (1980) diffusion model:

$$J_s = -D_s \phi \frac{\partial C}{\partial z}$$

where

$D_s = D_0 \phi$ (assumed $f \approx \phi^{-2}$)

ϕ= mean measured porosity

$\frac{\partial C}{\partial z}$ = change in vertical concentration gradient

The whole sediment diffusion coefficient, D_s, was calculated by correcting the free-solution diffusion coefficients for the

Table 1. Flux values calculated using Berner's (1980) diffusion model. These stations represent a transect through the oxygen minimum zone. Diffusion coefficients were calculated from the listed sources.

		μM /m² /d	μM /m² /d	nM /m² /d	μM /m² /d	mM /m² /d	mM /m² /d
Station	Depth(m)	Mn	Cu	Co	Fe	DOC	O2
11(E)	100	0.604	0.826	5.905	7.605	0.058	-0.322
17(I)	99	0.243	0.020	13.281	0.318		-0.187
6(C)	235	0.180	0.127	3.025	0.866		-0.379
5(B)	500	-0.035	-0.082	-0.214		-0.016	-0.422
7(L)	642	0.022	0.000	0.487		-0.072	-0.315
12(K)	1010	0.024	0.027	0.197	0.636	0.033	-0.135
10(M)	2000	0.229	0.066	1.260	0.203		-0.486

Free solution diffusion coefficients (D_0)

Li and Gregory, 1974

Mn^{2+} - 3.05×10^{-6} cm^2/sec
Co^{2+} - 3.41×10^{-6} cm^2/sec
Cu^{2+} - 3.41×10^{-6} cm^2/sec

Reimers and Smith, 1986

O_2 - 1.24×10^{-5} cm^2/sec

Robinson and Stokes, 1959

NH_3 - 1.66×10^{-5} cm^2/sec

effects of tortuosity with an estimated formation resistivity factor ($f \approx \phi^{-2}$). Free-solution diffusion coefficients, D_0, were taken from Li and Gregory (1974). Complex depth dependent terms for compaction and porosity were not included since these factors generate errors of 4% or less in flux calculations (Klump and Martens, 1989). Therefore, a measured value of the porosity in the top 1 cm of sediment was used for each station.

The pattern of trace metal fluxes obtained by this method is contrary to earlier notions that metal fluxes should be the highest from reducing sediments in the oxygen minimum zone. Trace metal fluxes appear to be the lowest in the oxygen minimum zone and increase as bottom water oxygen increases (Fig. 7). The fact that the gradients used for these flux calculations are from the near-interface oxic region of the sediments again points to processes other than reduction of metal oxides, unless the reductions are occurring in anoxic micro-environments. It seems feasible to suggest that trace metal fluxes from the California continental margin could be due to the remineralization of organic carbon carrier phase under oxic conditions, with an associated release of organically bound metals.

If trace metal fluxes are dependent on oxic organic remineralization, the organic carbon sedimentary signature should indicate lower remineralization rates in the oxygen

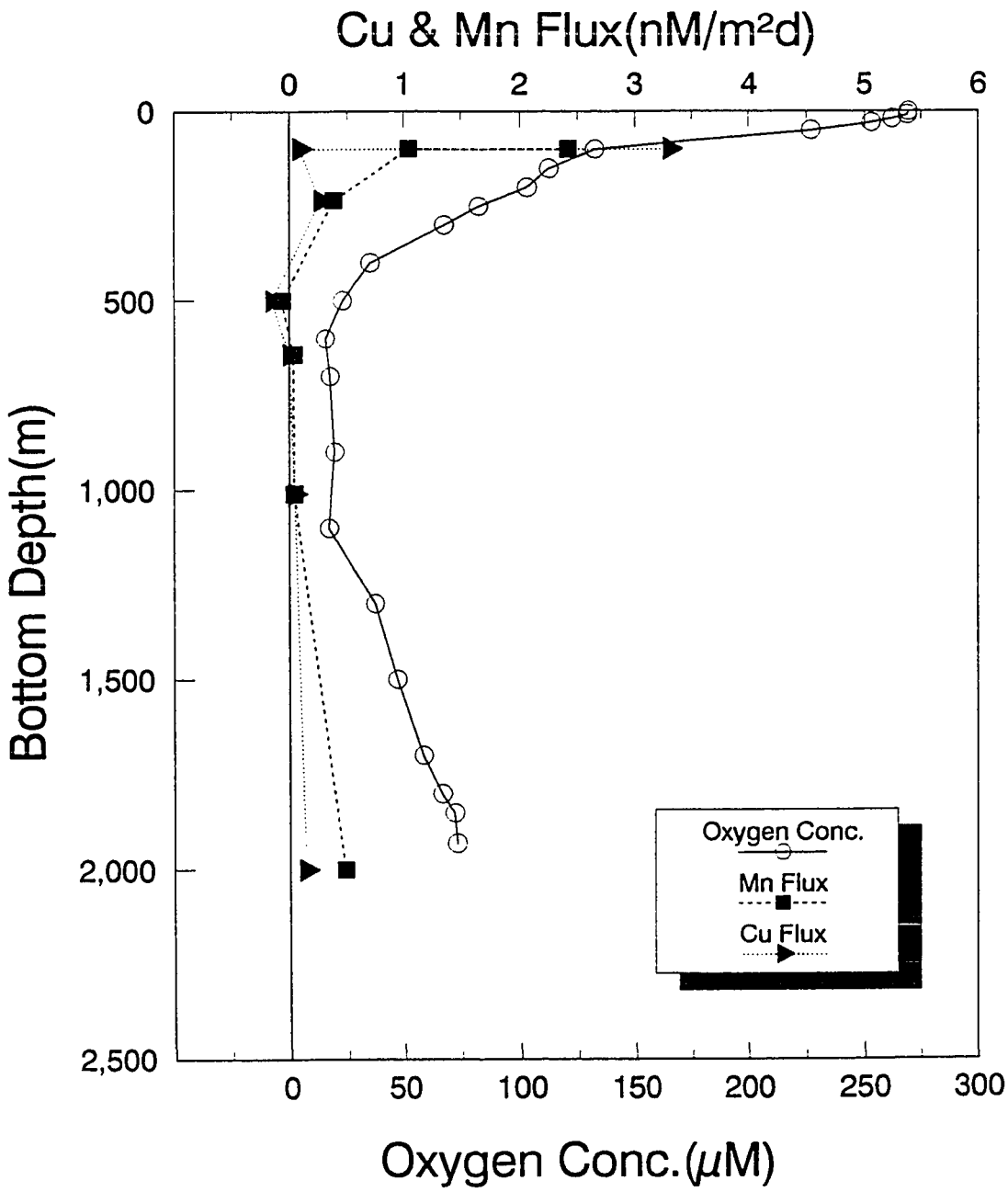

Figure 7) Modeled copper and manganese fluxes along a transect through the oxygen minimum. Oxygen values were from Winkler titrations of hydrocast samples at the 2000 m station.

minimum zone, since previous studies have shown that carbon remineralization occurs most rapidly at higher oxygen conditions (Jahnke et al., 1990). The enhanced preservation of organic carbon, seen in the superficial sediments of stations with low bottom water concentrations (Fig. 8), also seems to support this.

The results from this study show that whole core squeezing techniques can be useful in the analysis of trace metals near the sediment-water interface of marine sediments. The small sample volumes required to perform the flow injection analytical techniques allow multi-element and nutrient analysis while maintaining sampling depth resolution on the order of 1 millimeter. Profiles of metals in pore waters are used to evaluate diagenetic mechanisms controlling the mobility of trace metals from sediments of the California continental margin. Results indicate that trace metal fluxes are highest from sediments outside the oxygen minimum region. Remineralization of organic matter under oxic conditions and subsequent release of bound metals is the proposed mechanism.

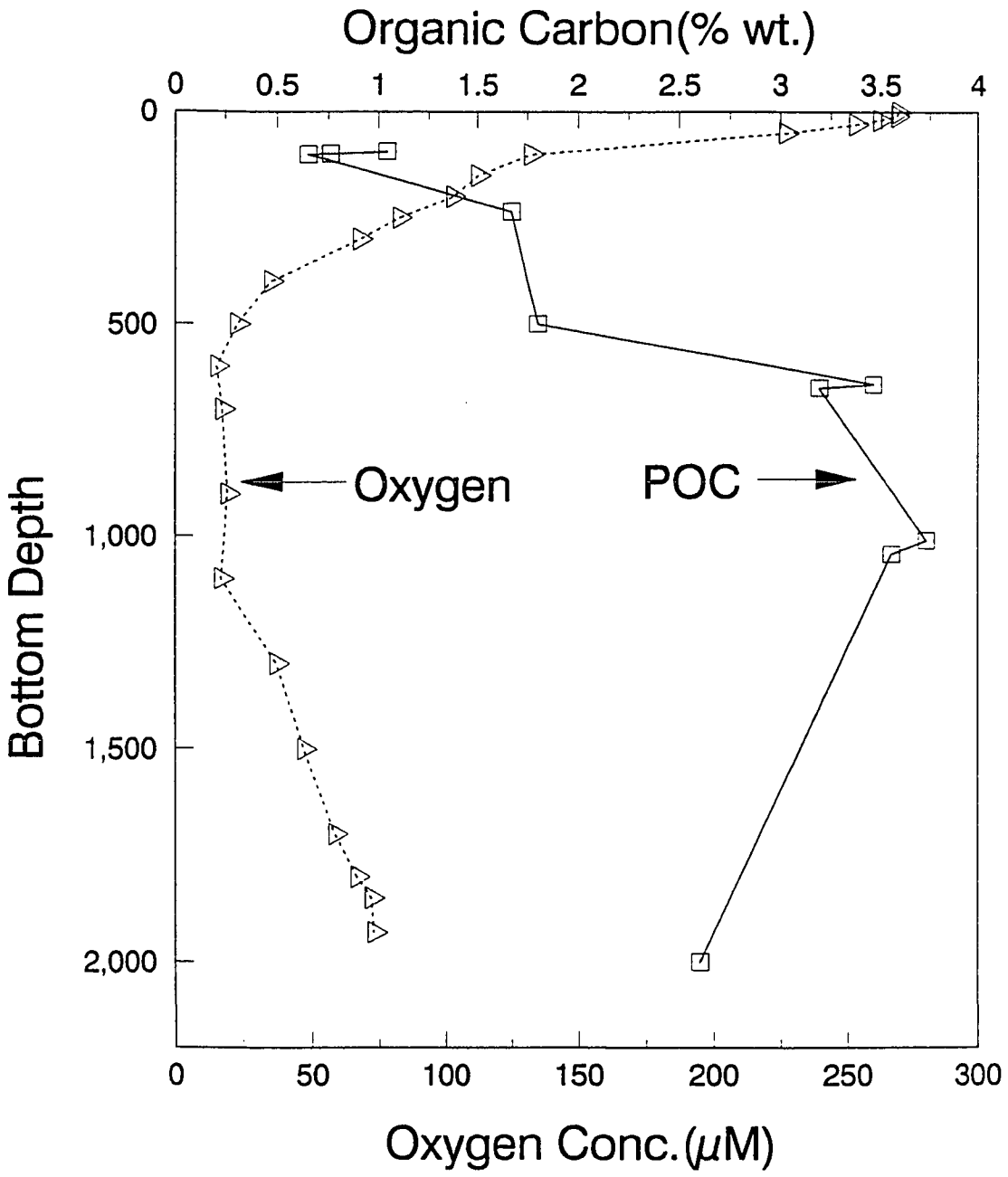

Figure 8) Particulate organic carbon from solid phase samples. Oxygen values were from Winkler titrations of hydrocast samples at the 2000 m station.

References

Bender, M., Martin, W., Hess, J., Sayles, F., Ball, L. and Lambert, C. (1987) A whole core squeezer for interfacial pore water sampling. Limnol. Oceanogr., **32**, 1214-1225.

Berelson, W.M. and Hammond, D.E. (1986) The calibration of a new free-vehicle benthic flux chamber for use in the deep sea. Deep Sea Research, **33(10)**, 1439-1454.

Berner, R.A. (1980) Early Diagenesis: A Theoretical Approach. Princeton, NJ: Princeton University Press

Chapin, T.P., Johnson, K.S., and Coale, K.H. (1991) Rapid determination of manganese in seawater by flow-injection analysis with chemiluminescence detection. Analytica Chimica Acta, **249**, 469-478

Chester, R. (1990) Marine Geochemistry: Sediment interstitial water and diagenesis. Unwin Hyman Ltd., Winchester, Mass.

Coale, K.H., Stout, P.M., Johnson, K.S. and Sakamoto-Arnold, C.M. (1992) Shipboard determination of copper in seawater using flow injection analysis with chemiluminescence detection. Anal. Chim. Acta (in press)

Elrod, V.A., Johnson, K.S. and Coale, K.H. (1991) Determination of subnanomolar levels of Iron(II) and total dissolved iron in seawater by flow injection

analysis with chemiluminescence detection. Analytical Chemistry **63**, 893-898

Emerson, S., Grundmanis, V., and Graham, D. (1980) Early diagenisis in sediments from the eastern equatorial Pacific. 1. Pore water nutrient and carbonate results. Earth Planet. Sci. Lett., **43**, 57-80

Froelich, P.N., Klinkhammer, G.P., Bender, M.L., Luedtke, N.A., Heath, G.R., Cullen, D., Dauphin, P., Hammond, D., Hartman, B., and Maynard, V. (1979) Early oxidation of organic matter in pelagic sediments of the eastern equatorial Atlantic: suboxic diagenisis. Geochim. Cosmochem. Acta., **43**, 1075-1090

Gordon, Jr., D.C. (1971) Distribution of particulate organic carbon and nitrogen at an oceanic station in the central Pacific. Deep Sea Research, **18**, 1127.

Heggie, D., Kahn, D. and Fisher, K. (1986) Trace metals in metalliferous sediments, MANOP Site M: interfacial pore water profiles. Earth and Planet. Sci. Lett., **80**, 106-116

Honeyman, B.D. and Santschi, P.H. (1988) Metals In Aquatic Systems. Environ. Sci. Technol., **22(8)**, 862-871

Jahnke, R.A. (1988) A simple reliable and inexpensive pore-water sampler. Limnol. Oceanogr., **33**, 483-487

Jahnke, R.A., Reimers, C.E. and Craven, D.B. (1990) Intensification of recycling of organic matter at the

sea floor near ocean margins. Nature, **348**, 50-54

Johnson, K.S., Stout, P.M., Berelson, W.M., and Sakamoto-Arnold, C.M. (1988) Cobalt and Copper distributions in the waters of Santa Monica Basin, California. Nature, **332**, 912-914

Klinkhammer, G. (1980) Early diagenesis in sediments from the eastern equatorial Pacific, II. Pore water results. Earth Planet. Sci. Lett., **49**, 81-101.

Klinkhammer, G., Heggie, D.T. and Graham, D.W. (1982) Metal diagenesis in oxic marine sediments. Earth Planet. Sci. Lett., **61**, 211-219.

Klump, J.., and Martens, C.S. (1989) The seasonality of nutrient regeneration in an organic-rich coastal sediment: Kinetic modeling of changing pore-water nutrient and sulfate distributions. Limnol Oceanogr., **34(3)**, 559-577

Lerman, A. (1979) Geochemical Processes. Water and sediment environments. New York: Wiley

Li, Y.H. and S. Gregory (1974) Diffusion of ions in sea water and deep-sea sediments. Geochim. Cosmochim. Acta, **38**, 703-714.

Nyffeler, Y.P., Santschi, P.H. and Li, Y-H. (1986) The relevance of scavenging kinetics to modeling of sediment-water interactions in natural waters. Limnol. Oceanog., **31(2)**, 277-292

Reimers, C.E. and Smith, K.L. (1986) Reconciling measured and predicted fluxes of oxygen across the sediment-water interface. Limnol. Oceanogr., **31(2)**, 305-318

Reimers, C.E. (1987) An in-situ microprofiling instrument for measuring interfacial pore water gradients. Deep-Sea Research, **31**, 305-318

Saager, P.M., Sweerts, J-P., and Ellermeijer, H.J. (1990) A simple pore water sampler for coarse sandy sediments of low porosity. Limnol. Oceanogr., **35(3)**, 747-751

Sakamoto-Arnold, C.M. and Johnson, K.S. (1987) Determination of picomolar levels of cobalt in seawater by flow injection analysis with chemiluminesence detection. Analyt. Chem., **59**, 1789-1794

Sayles, F.L. and Dickinson, W.H. (1991) The ROLAI^{2}D lander: a benthic lander for the study of exchange across the sediment-water interface. Deep-Sea Research, **38(5)**, 505-529

Sawlan, J.J. and Murray, J.W. (1983) Trace metal remobilization in the interstitial waters of red clay and hemipelagic marine sediments. Earth Planet. Sci. Lett., **64**, 213-230.

Shaw, T.J., Gieskes, J.W., and Jahnke, R.A. (1990) Early diagenesis in differing depositional environments: The response of transition metals in pore water. Geochim. Cosmochim. Acta, **54**, 1233-1246.

Soutar, A., Johnson, S., Fisher, K., and Dymond, J. (1981) Sampling the sediment-water interface for an organic rich surface layer. Trans. Am. Geophys. Union, **62**, 905

Strickland, J. and Parsons, T. (1972) A Practical Handbook For Seawater Analysis. Ottawa, Canada, Canadian Fisheries Research Board.

Wilson, T.R.S., Thomson, J., Hydes, D.J., Colley, S., Culkin, F. and Sorenson, J. (1986) Oxidation Fronts in Pelagic Sediments: Diagenetic Formation of Metal-Rich Layers. Science, **232**, 972-974

CHAPTER 3

Remineralization and Early Diagenesis of Copper In Sediments Near the Los Angeles County Sewage Outfalls

Abstract

Copper fluxes from coastal sediments were calculated from dissolved copper gradients in sediment pore waters and directly measured with a free vehicle benthic flux chamber, near the sewage outfalls of the L.A. County, California, Joint Water Pollution Control Project (JWPCP). Dissolved copper fluxes, determined by both methods, were in the range of 4 to 11 $\mu mol/m^2/d$. In contrast, the copper fluxes were 0.8 $\mu mol/m^2/d$ from sediments in Monterey Bay and 0.03 $\mu mol/m^2/d$ from sediments off Point Piedras Blancas. The high flux values found near the outfalls represent approximately 66% of the total effluent copper entering the ocean from the outfall diffusers. This estimate is much higher than obtained previously, but is consistent with recent studies in pelagic sediments. Trace metal concentrations and fluxes indicate a shallow (< 1 cm) dynamic region where trace metal mobility and recycling plays a major role in the preservation of solid phase copper in the outfall sediments.

Introduction

The Southern California Bight is under the increasing burden of 16 municipal wastewater facilities servicing the industrial and domestic needs of the region's 15 million people. The largest of these inputs is from outfall diffusers of the Joint Water Pollution Control Plant (JWPCP) located in 60 m of water off the Palos Verdes Peninsula. This plant services Los Angeles county and in 1988 was responsible for a wastewater flow of 375 million gallons per day (1.42×10^9 liters/day), of which 48% receives advanced primary treatment and 52% receives secondary treatment. Mass emissions of suspended solids have ranged from 170,000 metric tons/year in the early seventies to 36,300 metric tons/year in 1988 (SCCWRP, 1986-1989). Wastewater derived particles exhibit metal concentrations two to three orders of magnitude higher than seen in natural marine sediments (Bruland, 1974; Galloway, 1978).

The diagenetic fate of the metal-particle association during and after deposition is the subject of ongoing research. Early studies indicated that remineralization and mobilization of heavy metals was minimal in anaerobic organic rich sediments such as those adjacent to wastewater outfalls (Morel et al., 1975). A key point to Morel's argument was that deposition of sediments occurred within 24 hours of expulsion from the outfall diffusers. Since metal mobilization was not

believed to occur in anaerobic sediments, remineralization must occur in the first 24 hours, to be significant. Solid phase analysis and mass balance calculations of sediments adjacent to the JWPCP outfall indicated that less than 10% of the metals found in wastewater were incorporated into local sediments (Galloway, 1978). It followed that most particulate metals injected into the ocean from the JWPCP system were not deposited in the adjacent sediments, but were instead transported out to sea by coastal currents. The critical review of published data by Katz and Kaplan (1981) supported this view, yet they felt tenuous in their synthesis since little data was available on dissolved heavy metals in the interstitial waters near the Southern California outfalls. This lack of data was due in part to difficulties associated with the extraction of pore waters, in combination with the analytical and contamination problems associated with the small sample volumes.

In contrast to the early studies of polluted coastal sediments, the view that has emerged for trace metal cycling in the unperturbed deep-sea sediments emphasizes the release of dissolved metals from the sedimentary particulate phase. Studies of dissolved copper in the pore waters of oceanic sediments have demonstrated enrichments near the sediment-water interface (Klinkhammer et al., 1982; Sawlan and Murray, 1983; Heggie et al., 1986). Fluxes estimated from these

dissolved copper measurements indicated oxidation of particulate organic matter near the sediment-water interface, with an associated release of organically bound copper. This suggested that some metal-particle associations are strongly influenced by diagenetic processes and that extensive cycling occurs before burial (Finney and Huh, 1988).

The differences between these two views of metal cycling (metal-rich particle advection vs near-interface metal remineralization) led us to re-examine the cycle of copper at the sediment water interface in the JWPCP outfall region. Samples were collected from three stations on two separate occasions using both benthic flux chamber (Berelson and Hammond, 1986) and whole core squeezer techniques (Bender, et al., 1987). Samples were also collected from a shallow site in Monterey Bay and an open ocean site off Pt. Piedras Blancas for comparison of the outfall site to other ocean regimes. The present study is the first known attempt to address the pore water chemistry and diagenetic processes which lead to trace metal fluxes in the outfall region.

Sampling and Analytical Procedures

The sediments and overlying water column were sampled at three sites (Fig.1), chosen for their representation of the historical sedimentary trace metal gradient (Galloway, 1979;

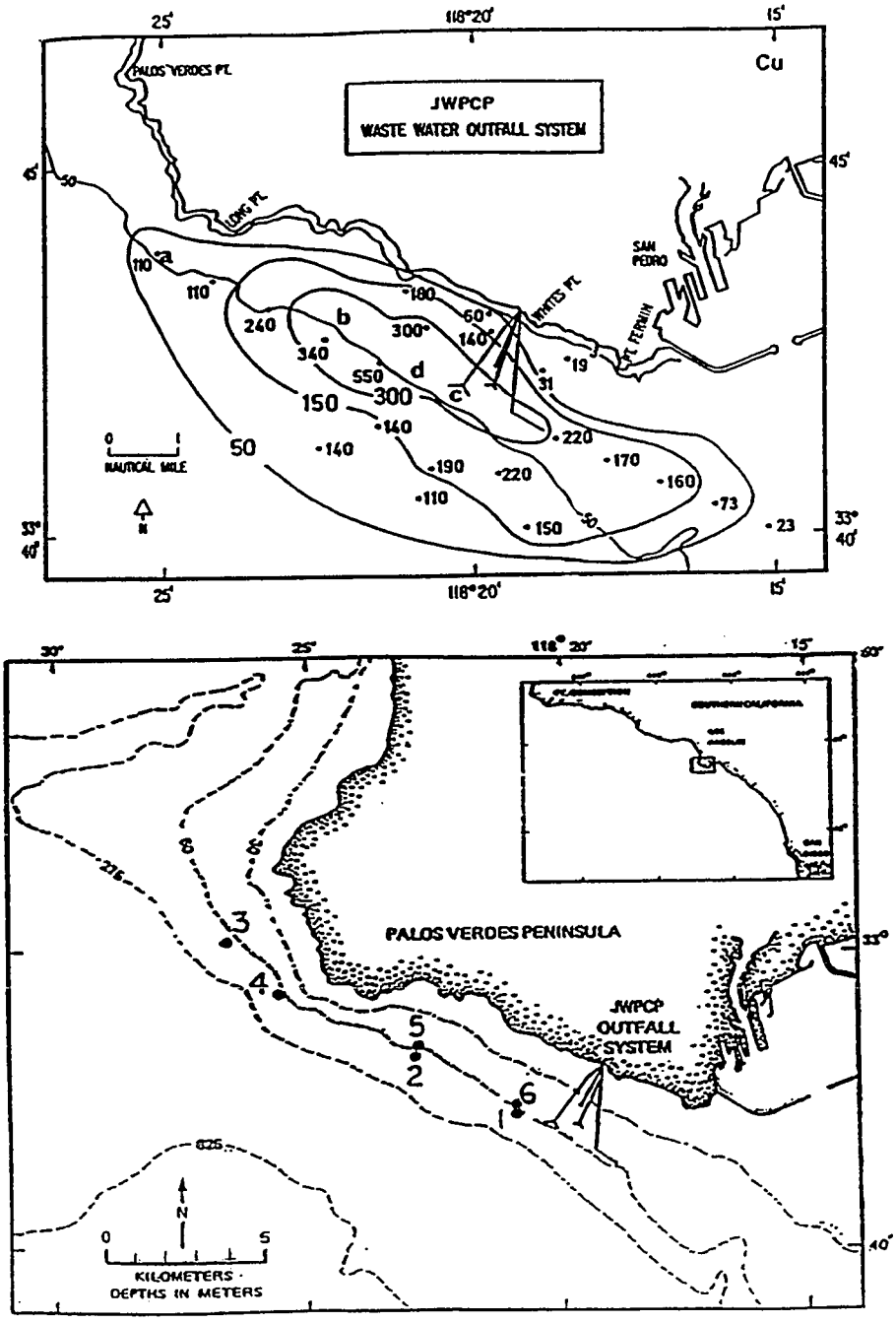

Figure 1) (a) Historic distribution of solid phase Cu in the surface sediment adjacent to the JWPCP outfalls after Galloway (1979). (b) Location of sampling stations 1-6, occupied in Feb. and Sept., 1991

Hershelman, et al., 1981). This solid phase trace metal signature is created by a general northwesterly flow of the prevalent bottom current, below the thermocline. Sampling stations 1 & 6 are located at the JWPCP outfall diffusers, stations 3 & 4 at a site ≈12 km north of the outfall and stations 2 & 5 at a site midway between the two. Sampling periods were in February (Stns. 1,2,3) and September (Stns. 4,5,6) of 1991. Sediment pore waters were extracted and analyzed to estimate metal fluxes across the sediment-water interface. Benthic flux chambers were deployed at each site to directly measure these fluxes.

Sediment Cores

Sediments were collected with a 30 cm^2 boxcore near the outfalls and with 1250 cm^2 boxcore at Monterey Bay and Pt. Piedras Blancas. Subcores were taken at sea with special attention to avoiding trace metal contamination. Core tops were sampled for pore waters to a depth of 3 cm using modifications of the whole-core squeezing techniques of Bender et al., 1987. Modifications include utilization of a regulated pneumatic ram to provide a constant sample flow for in-line oxygen and pH sensors (Fairey et al., submitted). All surfaces in contact with sample were acid-cleaned plastics (acrylic, PVC, TFE, PE and PP). The core barrel i.d. of 10 cm allows extraction of ≈ 7 ml of sample for each millimeter of piston displacement, in high porosity sediments. Samples were

filtered in-line (0.45 μm) during squeezing, and analyzed for nutrients using standard colorimetric techniques (Strickland and Parsons, 1972). The trace metals copper, manganese and cobalt were determined using flow injection analysis with chemiluminescence detection (FIA-CL)(Coale et al., in press; Chapin et al., 1991; Sakamoto-Arnold et al., 1987). Prior to the FIA-CL analysis, subsamples were diluted (1+25) with purified Millipore Milli-Q water (MQ-water). Sediment solid phase samples were sectioned at 2 mm intervals and analyzed for porosity, organic carbon and organic nitrogen. Porosity is expressed as per cent water, by volume, assuming a dry bulk density of 2.6 g/cm^3 and a porewater salinity of 35‰. Organic carbon and nitrogen in the solid phase were determined with a Perkin Elmer 440 Elemental Analyzer and are expressed as a percentage of total sample weight.

Benthic Lander

A free vehicle benthic lander (Berelson and Hammond, 1986) was deployed at each site to directly measure the flux of nutrients and trace metals from the sediments. Sediments were incubated in-situ, under stirred benthic flux chambers, as a time series of six aliquots of water was collected from each of three chambers at preprogrammed intervals. Samples were filtered (0.45 μm) prior to analysis. Oxygen concentrations inside and outside of the chambers were continuously monitored with a pulsed oxygen electrode

(Berelson et al., 1987). Sample aliquots were analyzed for nutrients and metals as stated for pore waters. Subsamples were diluted (1+7.5) with MQ-water prior to trace metal analysis.

Results and Discussion

Copper, manganese and cobalt concentrations, measured in pore waters along a transect at the outfalls, are shown in Figure 2. Although measured metal concentrations in pore waters were generally lowest at the site farthest north of the outfall (Stn.4), it should be noted that these levels still represent a 10-100 fold enrichment above the levels found in the pore waters of other ocean stations (Fairey et al., submitted; Heggie et al., 1986; Sawlan and Murray, 1983). Concentrations of copper in pore waters reached 1.8 μM (at 35 mm depth) at Stn. 4, while the highest measured copper values were found at the outfall site (9.8 μM at 35 mm depth). In comparison, dissolved copper concentrations in the pore waters of sediments collected in Monterey Bay or off Pt. Piedras Blancas are much lower than observed at any of the stations off the Palos Verdes Peninsula (Fig. 3).

The vertical profiles of dissolved copper, measured in the pore waters of unperturbed sediments off Pt. Piedras Blancas and Monterey Bay, where anthropogenic inputs are much

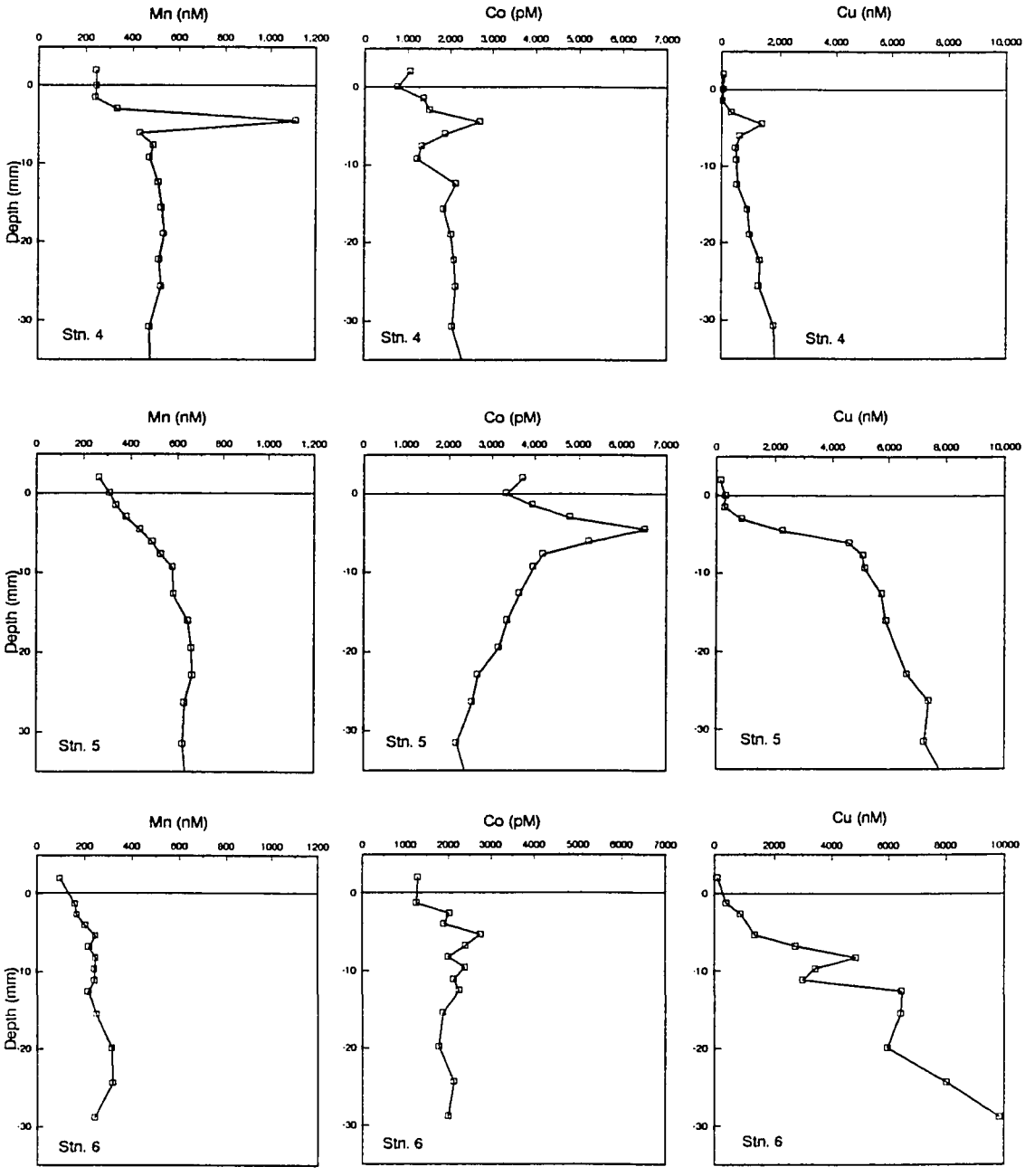

Figure 2) Profiles of Mn, Co, and Cu in pore waters as a function of sediment depth at Stations 4, 5, and 6 off the Palos Verdes Peninsula

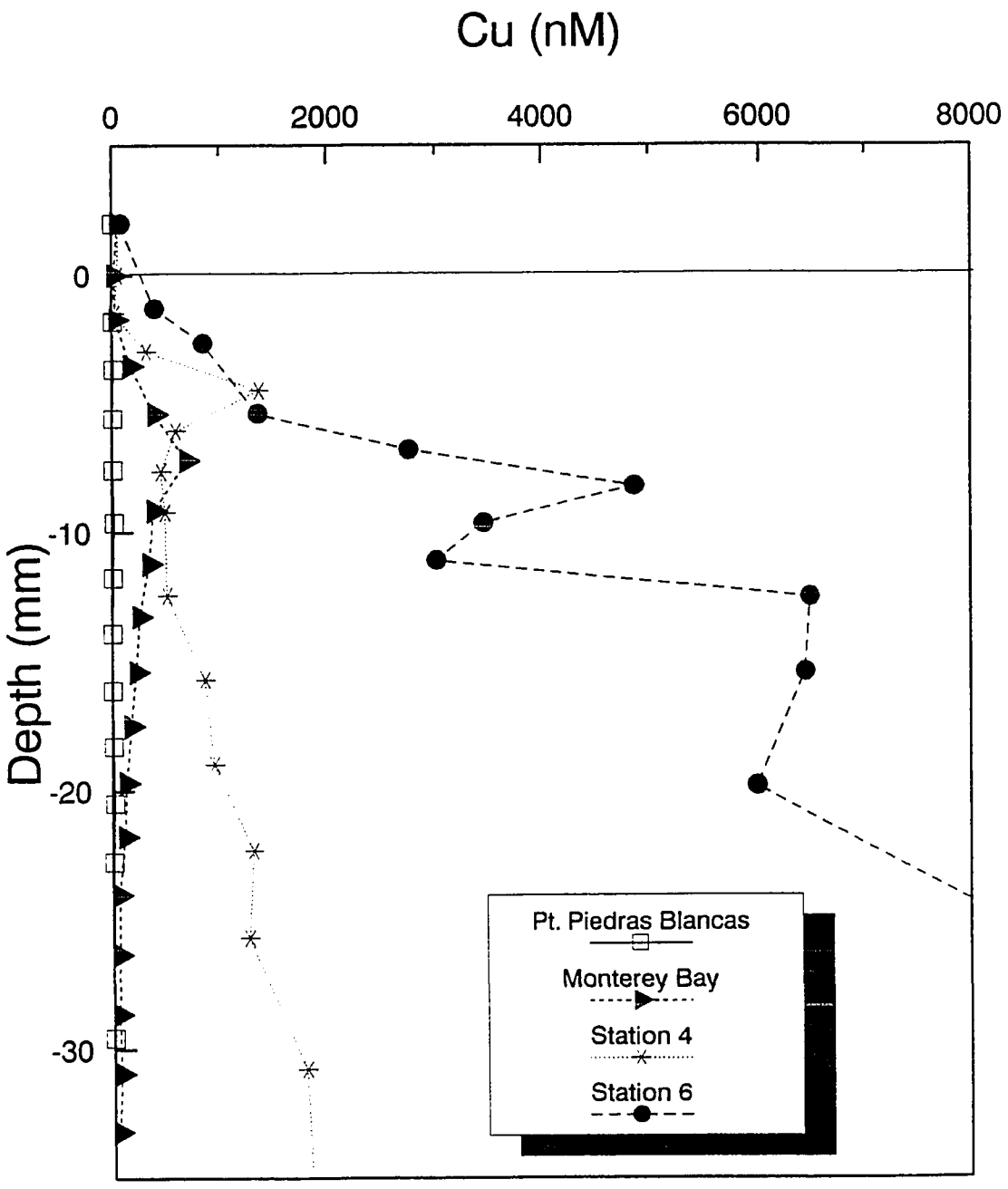

Figure 3) Copper profiles in pore waters of the JWPCP outfall region, Monterey Bay and Pt. Piedras Blancas.

lower, exhibit shallow concentration maxima and a smooth concentration decrease as depth increases in the sediments. These profiles are much like those observed in the deep-sea (Klinkhammer et al., 1982 and Shaw et al., 1990) where the maxima are attributed to the release of bound copper, during remineralization of particulate organic matter (POM), within the shallow oxic region (Chester, 1991). The decrease in dissolved copper concentrations with depth probably reflects the adsorption of copper onto sold phase surfaces or the precipitation of copper polysulfide minerals, such as chalcocite or covellite (Emerson et al.,1983; Jacobs et al., 1985).

In contrast, measured concentrations of copper in pore waters from the Palos Verdes stations nearest the outfalls (Stns. 5 & 6), are much higher and increase continuously down the core to a maximum sampling depth of 35 mm. Previous studies have demonstrated a strong enrichment in sedimentary copper around the outfall (Galloway, 1979). The high POM content of the outfall sediments is demonstrated by solid phase particulate organic carbon measurements at Stn. 6 of 5% (by weight), in comparison to an average of less than 1% for the Monterey Bay and Pt. Piedras Blancas stations. The elevated copper concentrations in pore waters must reflect extremely high rates of remineralization of sewage derived POM, with an associated release of organically bound copper.

Decreases in organic carbon with depth indicate continued remineralization below the oxic front. This would occur in concert with the predicted diagenetic series proposed for anoxic sediments, through utilization of secondary oxidants such as NO_3^-, MnO_2, Fe_2O_3 and SO_4^{2-} (Froelich et al.,1979; Berner, 1980; Chester, 1991). Sulfide concentrations of up to 20 mM have been measured in the top 5 cm of these sediments (J. Childress, personal comm.). Since copper is a class B metal ion with a very low solubility in the presence of sulfide the accumulation of large dissolved copper concentrations in the presence of sulfide was quite unexpected. However, Emerson et al. (1983) have shown that the formation of copper polysulfide complexes can lead to a marked increase in copper solubility at the range of total sulfide found in natural waters (1 to 6000 μM). Thermodynamic calculations indicate that micromolar concentrations of dissolved copper would be stable at sulfide concentrations approaching 1mM. High sulfide concentrations that result from the metabolic degradation of abundant sedimentary organic matter, by sulphate reducing bacteria, must account for the persistence of high dissolved copper concentrations in the sediments near the outfalls. The presence of sulfides may also be a possible explanation for the observed pH shifts (Fig. 4) seen in the suboxic pore waters as metal-sulfide complexes are formed.

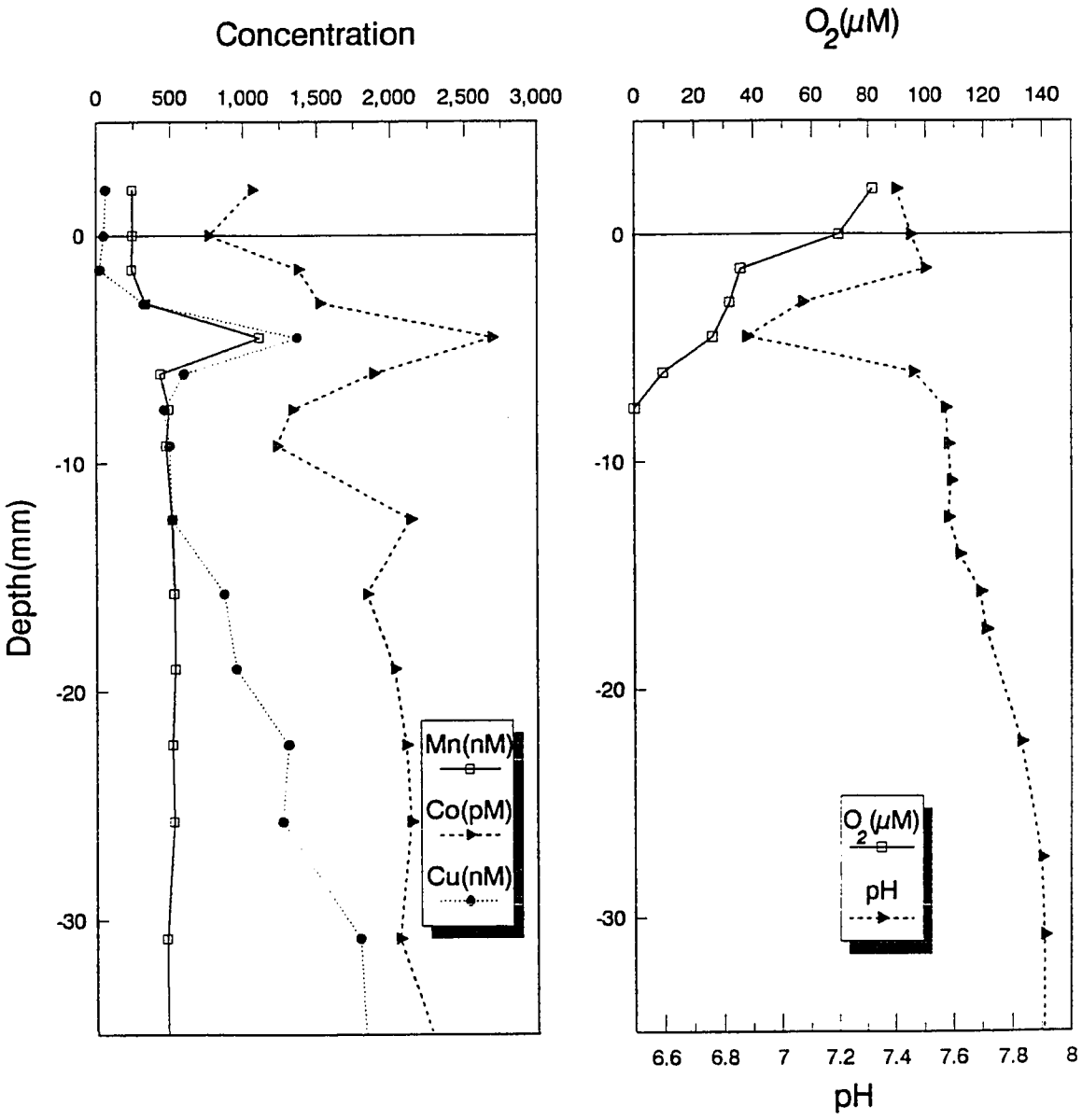

Figure 4) (a) Pore water profiles of Mn, Co and Cu at Station (b) Pore water profiles of pH and oxygen at Station 4. pH was determined with a Sensorex electrode placed in-line with sample effluent. Oxygen was determined with an in-line polarographic oxygen sensor. Comparison of figures (a) and (b) indicate maximum trace metal remobilization at the same depth as the pH minimum, above the anoxic interface.

Interestingly, Stn. 4 exhibits a copper profile intermediate between those seen closer to the outfall and those seen in the more pristine sediments of northern California. A shallow (5 mm) copper maximum is still seen, although the general trend is a gradual increase in dissolved copper with depth. This profile may characterize less perturbed sediments where rapid near-surface remineralization of copper from organic matter is balanced by minor copper sulfide precipitation in the shallow oxic region.

The rapid remineralization of organic matter seen in these sediments results in a diagenetic flux of metals and nutrients across the sediment-water interface. We have used the measured pore water profiles and gradients to calculate flux values (J_s) for metals and nutrients at each station (Table 1), using Berner's (1980) diffusion model:

$$J_s = -D_s \phi \frac{\partial C}{\partial z}$$

where

$D_s = D_0 \phi$ (assumed $f \approx \phi^{-2}$)

ϕ = mean measured porosity

$\frac{\partial C}{\partial z}$ = change in vertical concentration gradient

The whole sediment diffusion coefficient, D_s, was calculated by correcting the free solution diffusion coefficient for the

Table 1. Calculated fluxes based on pore water gradients (C) as well as measured fluxes from the benthic flux chambers(L). Free-solution diffusion coefficients, used to calculate diffusion in sediments, and their referenced sources are given.

		uM/m^2/d	uM/m^2/d	nM/m^2/d	nM/m^2/d	uM/m^2/d	uM/m^2d
Station	Depth(m)	Mn(L)	Mn(C)	Co(L)	Co(C)	Cu(L)	Cu(C)
4	77	16.6	2.8	366	6.9	4.5	4.7
5	65	12.7	0.4	534	10.6	6.4	10.7
6	66	4.7	0.5	-7.4	5.7	5.2	4.9
Mont.Bay	100		0.6		5.9		0.8
Pled.Blan	99		0.2		13.2		0.02
		uM/m^2/d	uM/m^2/d	mM/m^2/d	mM/m^2/d	mM/m^2/d	mM/m^2d
Station	Depth(m)	NH_3(L)	NH_3(C)	PO_4(L)	PO_4(C)	O_2(L)	O2(C)
4	77	2.5		0.2			-0.34
5	65	4.5		0.6			-0.52
6	66	3.9		1.8			-1.18
Mont.Bay	100						-0.30
Pled.Blan	99						-0.10

Free solution diffusion coefficients (D_0)

Li and Gregory, 1974
Mn^{2+} - 3.05 x 10^{-6} cm^2/sec
Co^{2+} - 3.41 x 10^{-6} cm^2/sec
Cu^{2+} - 3.41 x 10^{-6} cm^2/sec

Reimers and Smith, 1986
O_2 - 1.24 x 10^{-5} cm^2/sec

Robinson and Stokes, 1959
NH_3 - 1.66 x 10^{-5} cm^2/sec

effects of tortuosity with an estimated formation resistivity factor ($f \approx \phi^{-2}$). Free-solution diffusion coefficients, D_0, were taken from the sources listed in Table 1. Complex depth dependent terms for compaction and porosity were not included since these factors generate errors of 4% or less in flux calculations (Klump and Martens, 1989). Therefore, a mean value of measured porosities from the top 1 cm was used for each station. The highest calculated fluxes from the outfall region were at the mid-station (Stn. 5) for copper (10.7 μmoles/m^2/d). Copper fluxes at Stn. 6 and Stn. 4 were 4.9 μmoles/m^2/d and 4.7 μmoles/m^2/d, respectively. In comparison to the outfall region, copper fluxes were considerably lower at Monterey Bay (0.8 μmoles/m^2/d) and Pt. Piedras Blancas (0.02 μmoles/m^2/d). Cobalt fluxes were also highest at Stn. 5 (10.6 nmoles/m^2/d) while the highest flux for manganese (2.8 μmoles/m^2/d) was from Stn. 4. The outfall station (Stn. 6) showed the largest flux of ammonia (1.3 μmoles/m^2/d).

Mean values for measured metal concentrations in the three benthic chambers, at Stns. 4, 5 & 6, are plotted versus time in Fig. 5. Linear regressions of the change in metal concentration, within the chambers over the duration of the deployment, are used to determine benthic fluxes at each station. Correlation coefficients (R^2) were >0.9 for manganese and cobalt, but scatter in the copper data only gave R^2 values of <0.6. The lander may have contaminated the benthic

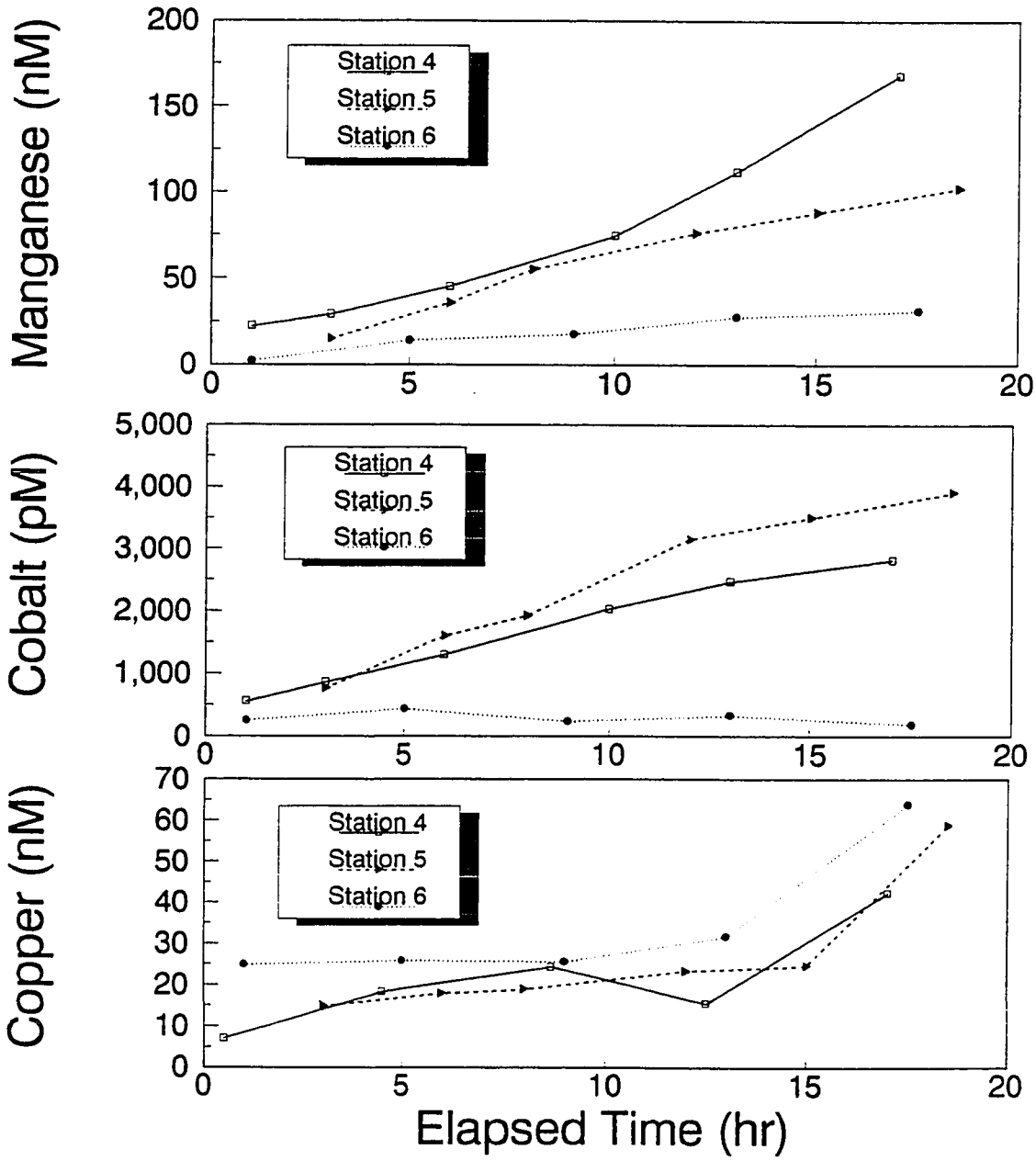

Figure 5) Benthic flux chamber metal concentrations over time during 24 hour deployments at Stations 4, 5 and 6. Slopes from the data were used to calculate metal fluxes reported in Table 1.

chamber samples with copper, because initial draws were often substantially higher in copper than the bottom water. This was not so for manganese and cobalt. We have not included any chamber data where the initial sampling values suggested contamination.

Benthic flux measurements determined with the lander are presented in Table 1. The copper fluxes determined with the lander agree well with the copper fluxes estimated from the pore water data. Copper fluxes appear to be driven by the regeneration of Cu from below the sediment-water interface where the highest copper concentrations are found. Stabilization of these high dissolved copper concentrations is realized by the formation of copper polysulfide complexes (Emerson et al., 1983). On the other hand, lander and pore water estimates of benthic flux do not agree for Mn and Co. We believe this discrepancy for Mn and Co arises because their remineralization is maximal in the sediment's fluff layer (Johnson et al., submitted); a region not easily sampled with a box corer. Gradients in pore waters may not be sampled with sufficient depth resolution to accurately estimate Mn and Co fluxes. Mn and Co are also further influenced by metal oxide interface cycling and show low solubility under high sulfide conditions. Estimates from pore water profiles therefore tend to underestimate the flux of these elements. Under these conditions it is reasonable to expect Mn and Co fluxes not to

agree for both methods.

Solid phase data is shown in Fig.6 and shows organic carbon, organic nitrogen and porosity all highest at the outfall station. Carbon/nitrogen ratios can be useful as indicators for the incorporation of sewage derived organic matter into sediments (Morel et al., 1975). Measured carbon/nitrogen ratios fall within the range of 11.6 - 29.7 reported for the outfall region by Sweeney et al. (1980) and the C/N ratio of 12:1 at the outfall station is similar to that of the reported discharge effluent at about 13:1. This supports Sweeney's conclusions that sediments near the outfalls are largely derived from wastewater particles. In contrast, the C/N ratio in sediments from Monterey Bay were 7:1 and 8:1 from Pt. Piedras Blancas, with the lower ratios reflecting a natural marine particle component. At mid-station 5, where copper and cobalt fluxes were the highest, the C/N ratio reaches 25:1. Changes in the C/N ratio can be attributed to the preferential utilization of proteins during bacterial degradation of organic matter (Gordon, 1971). It is difficult to estimate the extent of bacterial degradation by C/N ratios alone, but it appears that in sediments with higher C/N ratios the natural decomposition process has proceeded further than in sediments with lower ratios. Assuming the sedimentation rates are similar at all three stations, the high C/N ratios seen at Stn. 5 should reflect high rates of

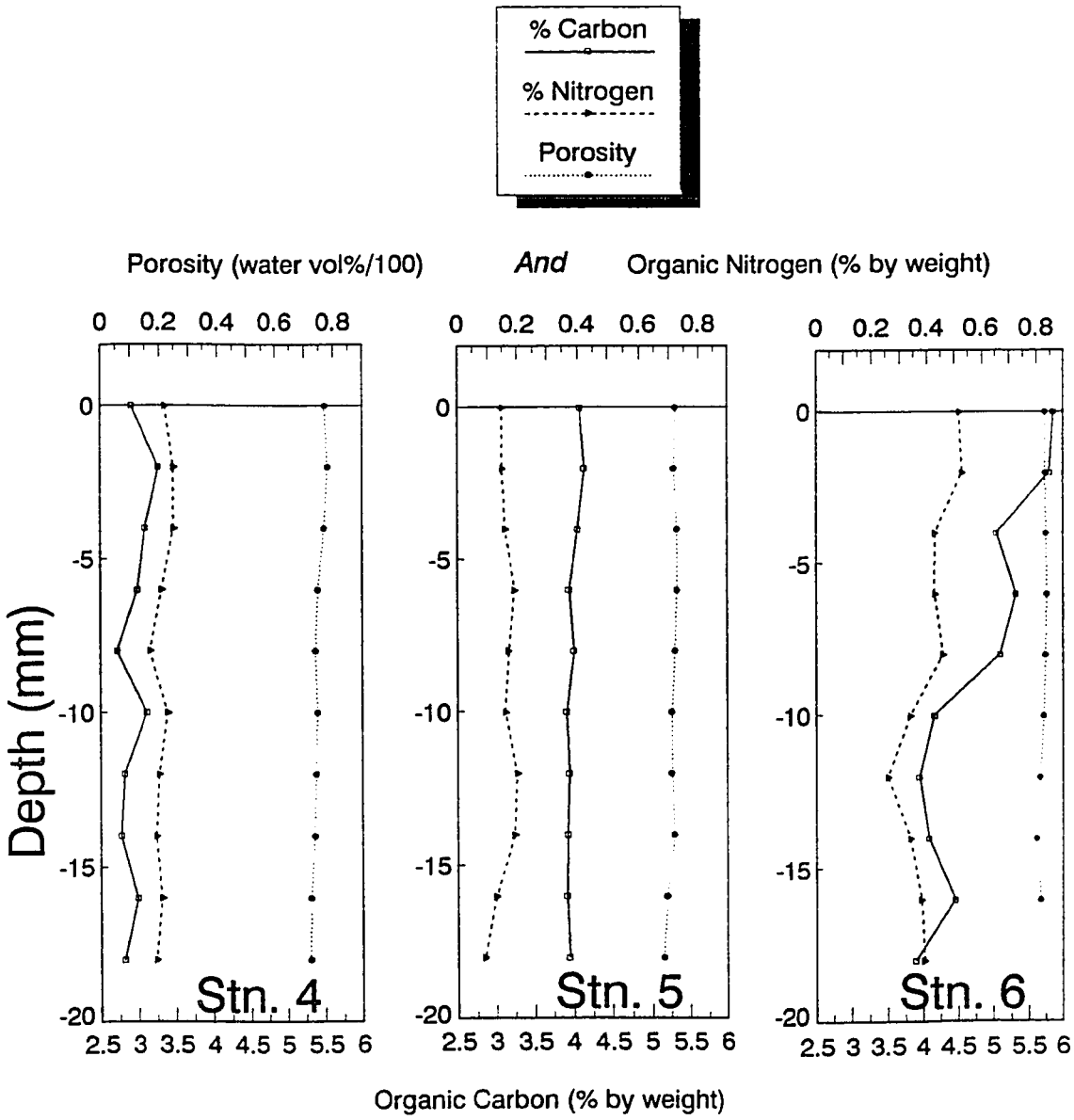

Figure 6) Solid phase carbon, nitrogen and porosity data from 2mm sections of sediment subcore. Porosity and organic nitrogen is expressed on the upper scale. Organic carbon is expressed on the lower scale. Porosity is expressed as % water, by volume, with an assumed density of the dry sediment at 2.6 g/cm^3, and salt corrected for 35‰. Organic carbon and nitrogen are shown as a percentage of total sample dry weight.

remineralization of organic matter, with an associated release of metals. This is supported by the correlation (r^2=0.89) between C/N ratios and copper fluxes for all stations off Palos Verdes, Monterey Bay and Pt. Piedras Blancas (Fig. 7). These factors lend support to the argument that the large copper fluxes from the outfall region are dependent on the remineralization of sewage derived organic carbon near the sediment-water interface.

To estimate the significance of these flux values, we constructed a copper budget for the JWPCP wastewater outfall region (Fig 8). For this model metals were assumed to be associated with settling particles over an area 20 km long and 5 km wide. This 100 km^2 area was chosen to encompass our study area and the region of superficial sediment enrichments of trace metals reported by Hershelman et al. (1981). The 1988 annual mass emissions for copper from the outfall (SCCWRP, 1986-1989) are used to calculate the flux of copper into the sediments as 8.3 $\mu moles/m^2/d$. Mean Cu fluxes out of the sediments, calculated from pore waters and flux chambers, are 5.5 ± 2.8 $\mu moles/m^2/d$ and 5.4 ± 0.8 $\mu moles/m^2/d$, respectively. An average flux determined from these two methods would account for remineralization of approximately 66% of the total effluent copper discharged on a daily basis. The fraction remineralized may actually be higher if some of the particulate copper is remineralized prior to settling.

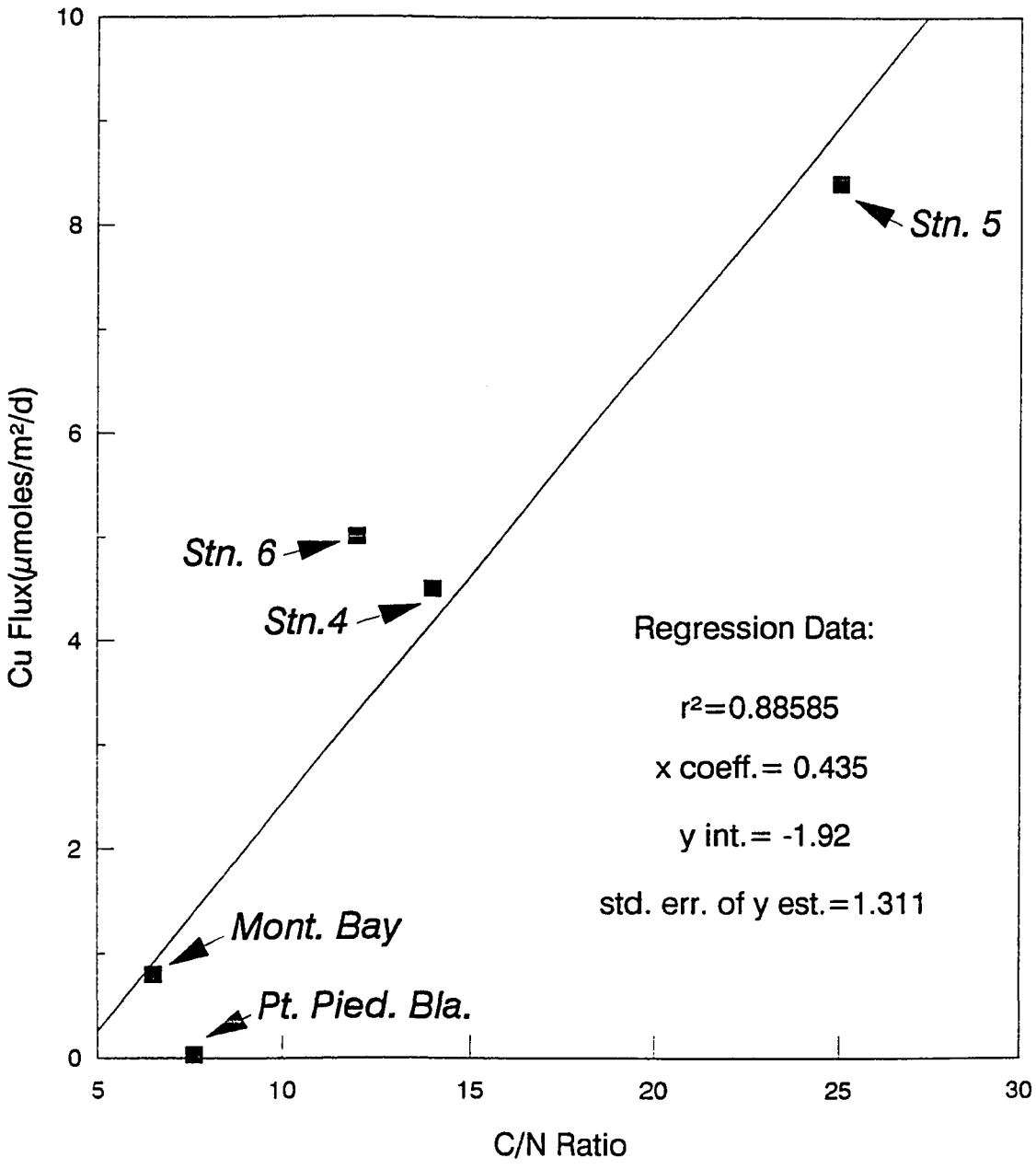

Figure 7) Average copper fluxes, calculated from lander and pore waters, vs carbon/nitrogen ratios at Whites Point, Monterey Bay and Pt. Piedras Blancas.

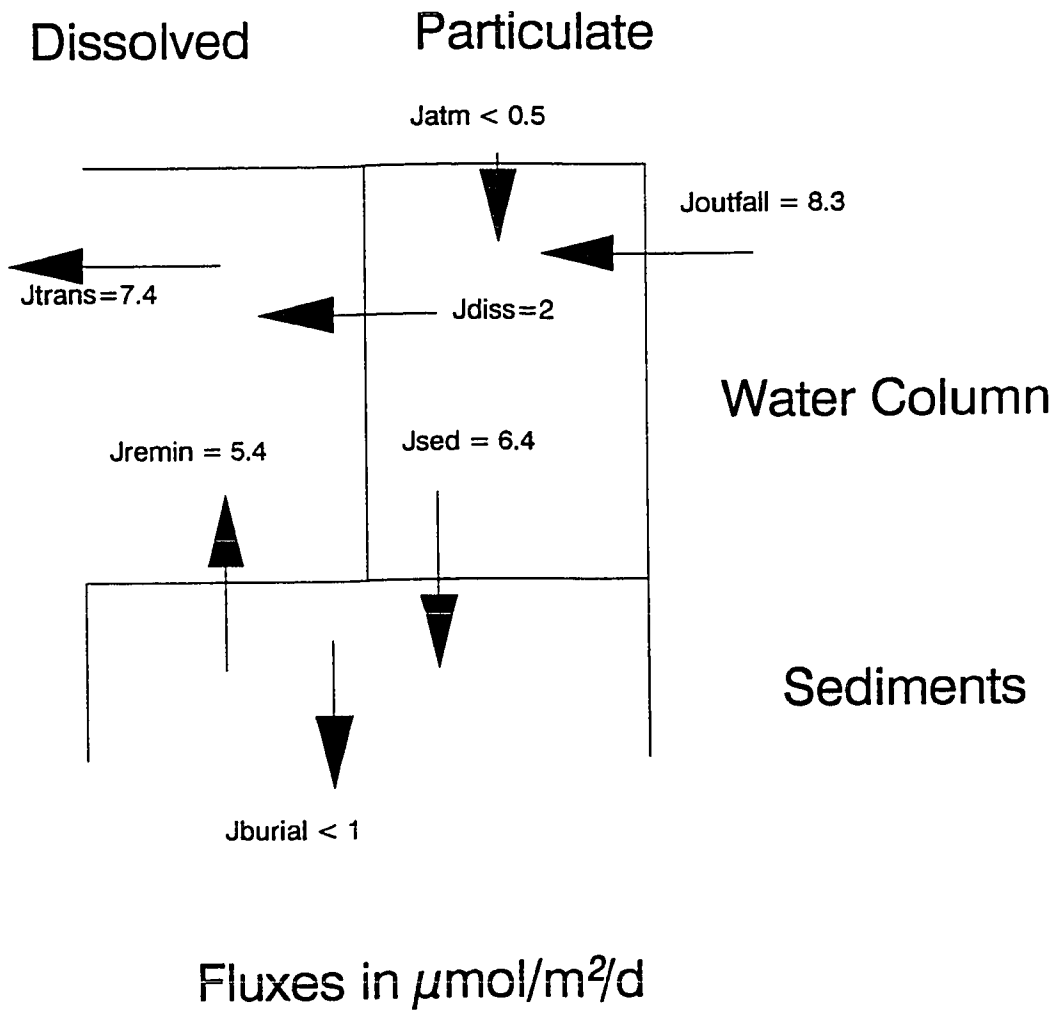

Figure 8) Copper budget for the 100 km² outfall region. All flux values are in μmoles/m²/d. $J_{outfall}$ was calculated by distributing total 1988 JWPCP effluent copper (SCCWRP, 1986-1989) over the outfall region. J_{diss} is calculated from Paulson et al. (1991) estimates that 25% of effluent copper is remineralized prior to settling. Atmospheric inputs are estimated from Chester (1991). Burial estimates are made from solid phase data of Galloway (1979) and Hershelman (1981). J_{remin} is an average flux value calculated from pore water gradients and benthic flux chamber measurements at sampling stations during February and September. J_{trans} is a net term from J_{diss} and J_{remin} estimating transport of copper out of the outfall region.

A recent study by Paulson et al. (1991) examined the remobilization of copper from marine particulate matter and from sewage. They found that when mixing primary sewage effluent with natural seawater, 40% of the dissolved copper was initially lost from solution due to flocculation, followed by remobilization of 25% of the total effluent Cu within 15 min to 4 days. This yielded remobilization rates from sewage which were about two orders of magnitude higher than that from natural marine organic matter.

If approximately 25% of total effluent Cu is remineralized from settling particles as suggested by Paulson et al. (1991), and approximately 66% is remineralized in pore waters as suggested by this study, then little copper would be retained in the solid phase. This could explain why solid phase studies (Galloway, 1979; Hershelman et al., 1981) found less than 10% of the effluent metals in the outfall sediments.

Intense recycling of copper at the sediment-water interface has been proposed in recent studies of metal geochemistry from open ocean sediments. Callender and Bowser (1980) found regeneration of copper from pelagic sediments of the northeastern Pacific to be > 90%. Klinkhammer (1980) estimated dissolved copper fluxes from sediments of the eastern Pacific to be near 100% of sedimentary inputs and in a later study (Klinkhammer et al., 1982) suggested that core top copper maxima indicated that diagenetic remobilization of

copper was restricted to a thin layer at the interface, where the most intense carbon remineralization occurs. Cu/carbon ratios were used by Sawlan and Murray (1983) to explain near surface copper enrichments as a result of aerobic oxidation of labile organic carbon. They suggested that this remineralization results in the recycling of 75% of the copper reaching the sediments. We believe a similar type of intense recycling, as proposed for these open ocean sediments, is also occurring in the organic rich sediments found off the Palos Verdes Peninsula.

The study by Shaw et al. (1990) suggests that metal mobility may include seasonal or event linked responses, and examination of the early results from this study indicate the possibility of seasonal fluctuations. Pore water Cu was analyzed both in Feb. and Sept. and a seasonal response of increased summer flux of copper is suggested by Figure 9. Sediment trap fluxes measured near the JWPCP outfall in 1986 and 1987 show a seasonal increase in particles during winter (SCCWRP, 1986-1989). An increase in metal flux might be expected, but the particle increase is from storm surge resuspension of sediments and storm runoff, both of which have low organic content. Distinct seasonal cycles in the remineralization of sedimentary organic matter has been described as a biological metabolic response to temperature oscillations (Klump and Martens, 1989), but the question of

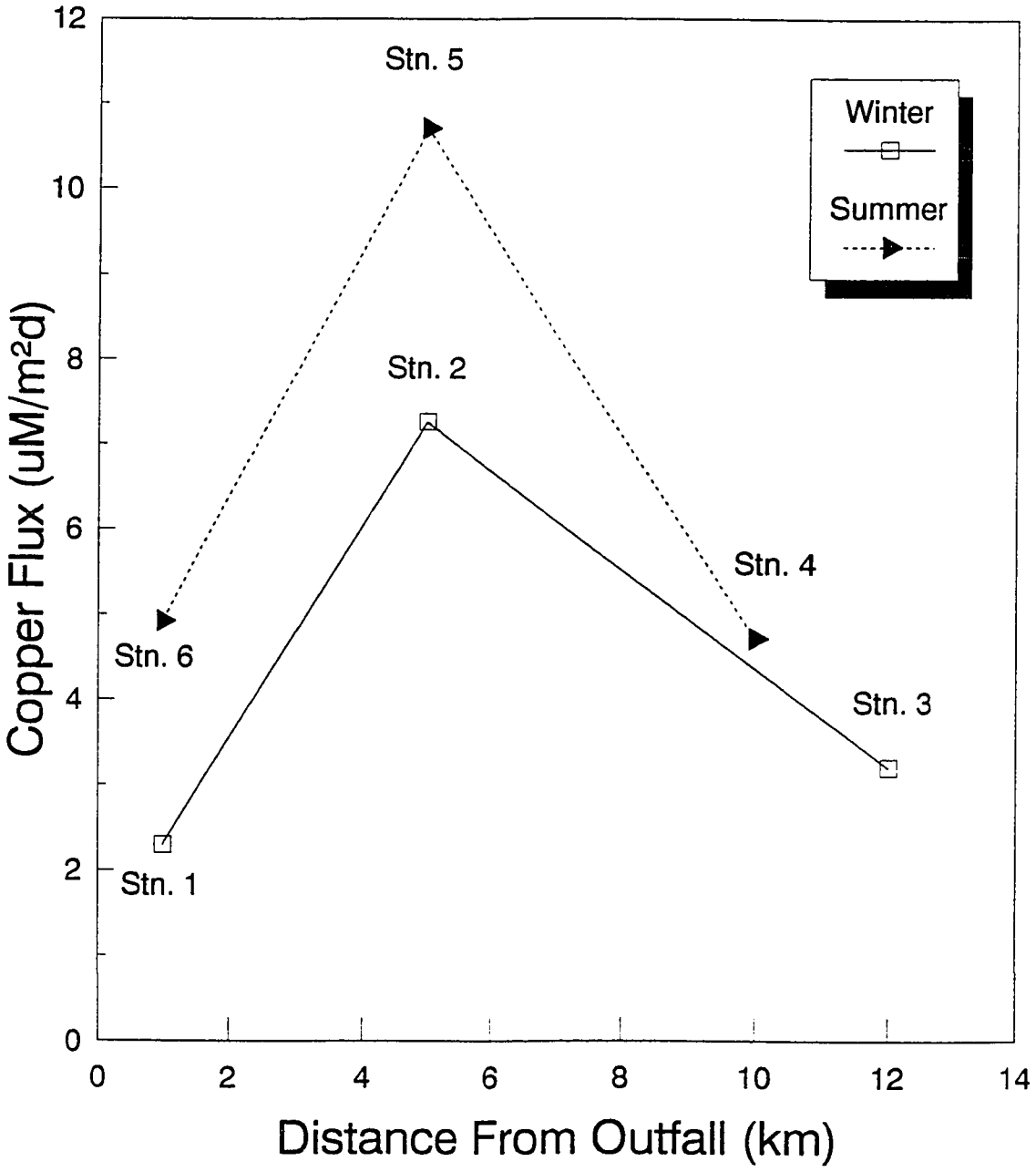

Figure 9) Seasonal comparison of modeled pore water copper fluxes on a transect north of the outfall diffusers.

possible decreases in metal fluxes during winter is an area still open for further study.

The value in this study comes from addressing the long standing paradigms that 1) Heavy metals from sewage outfalls are rapidly buried in sediments and 2) Metals are transported from the region with associated effluent particles. Our data contradicts these earlier theories and demonstrates large dissolved copper fluxes from outfall sediments. It is our belief that these fluxes are a result of oxic bacterial degradation of sewage particles with a subsequent release of the organically bound metal. These processes appear to be similar to those operating in deep-sea sediments. Much of the knowledge accumulated from studies of these pelagic systems may be applicable to studies of degraded coastal sediments such as occur off the Palos Verde Peninsula. This work begins to establish a pattern where trace metal mobility and recycling, from the sediment's superficial layer, plays a major role in the water column chemistry and sediment diagenesis of the outfall region. It is critical that future studies take notice of this shallow dynamic layer so that regulatory sewage treatment policies are made with full knowledge of trace metal mobility.

References

Bender, M., Martin, W., Hess, J., Sayles, F., Ball, L. and Lambert, C. (1987) A whole core squeezer for interfacial pore water sampling. Limnology and Oceanography, **32**, 1214-1225.

Berelson, W.M., and Hammond, D.E. (1986) The calibration of a new free-vehicle benthic flux chamber for use in the deep sea. Deep Sea Research, **33(10)**, 1439-1454

Berelson, W.M., Hammond, D.E., Smith, Jr.,K.L., Jahnke, R.A., Devol, A.H., Hinga, K.R. Rowe, G.T. and Sayles, F. (1987) In-situ benthic flux measurement devices: bottom lander technology. Marine Technology Society, **21**, 26-32.

Berner, R.A. (1980) Early Diagenesis: A Theoretical Approach Princeton, NJ: Princeton University Press

Bruland, K.W., Bertine, K., Koide, M. and Goldberg, E.D. (1974) History of Metal Pollution in Southern California Coastal Zone. Environ. Sci. & Technol., **8**, 425-32

Bruland, K.W., Franks, R.P., Knauer, G.A. and Martin, J.H. (1979) Sampling and analytical methods for the determination of copper cadmium, zinc and nickel at the nanogram per liter level in sea water. Analy. Chim. Acta, **105**, 223-245

Callender, E. and Bowser, C.J. (1980) Manganese and copper geochemistry of interstitial fluids from manganese-rich

pelagic sediments of the northeastern equatorial Pacific Ocean. Am. Jour. Sci. **280**, 1063-1096

Chapin, T.P., Johnson, K.S., and Coale, K.H. (1991) Rapid determination of manganese in seawater by flow-injection analysis with chemiluminescence detection. Analytica Chimica Acta, **249**, 469-478

Chester, R. (1990) Marine Geochemistry: Sediment interstitial water and diagenesis. Unwin Hyman Ltd., Winchester, Mass.

Coale, K.H. and Bruland, K.W. (1988) Copper complexation in the Northeast Pacific. Limnol. Oceanogr., **33**, 1084-1101

Coale, K.H., Stout, P.M., Johnson, K.S. and Sakamoto-Arnold, C.M. (1992) Shipboard determination of copper in seawater using flow injection analysis with chemiluminescence detection., Anal. Chim. Acta (in press)

Emerson, S., Grundmanis, V., and Graham, D. (1980) Early diagenisis in sediments from the eastern equatorial Pacific. 1. Pore water nutrient and carbonate results. Earth Planet. Sci. Lett., **43**, 57-80

Emerson, S., Jacobs, L. and Tebo, B. (1983) The behavior of trace metals in marine anoxic waters: solubilities at the oxygen-hydrogen sulfide interface. In Trace Metals in Sea Water. Wong, Boyle, Bruland, Burton, & Goldberg (eds.) Plenum Press, New York

Fairey, W.R., Johnson, K.S., Coale, K.H., Berelson, W.B. and Elrod, V.A. (1992) Trace metal analysis of sediment pore waters: A transect through the oxygen minimum of the California margin. Submitted

Finney, B.P. and Huh, C-A. (1989) History of Metal Pollution in the Southern California Bight: An Update. Environ. Sci. Technol., **23(3)**, 294-303

Froelich, P.N., Klinkhammer, G.P., Bender, M.L., Luedtke, N.A., Cullen, D., Dauphin, P., Hammond, D., Hartman, B., and Maynard, V. (1979) Early oxidation of organic matter in pelagic sediments of the eastern equatorial Atlantic: suboxic diagenesis. Geochim. Cosmochim. Acta, **49**, 1075-1090

Galloway, J.N. (1978) Alteration of trace metal geochemical cycles due to the marine discharge of wastewater. Geochim. Cosmochim. Acta, **43**, 207-208

Gordon, Jr., D.C. (1971) Distribution of particulate organic carbon and nitrogen at an oceanic station in the central Pacific. Deep Sea Research, **18**, 1127.

Hershelman, G.P., Schafer, H.A., Jan, T.K., Young, D.R. (1981) Metals in marine sediments near a large California municipal outfall. Marine Pollution Bulletin, **12(4)**, 131-134.

Heggie, D., Kahn, D. and Fisher, K. (1986) Trace metals in metalliferous sediments, MANOP Site M: interfacial pore

water profiles. Earth and Planet. Sci. Lett., **80**, 106-116

Honeyman, B.D. and Santschi, P.H. (1988) Metals In Aquatic Systems. Environ. Sci. Technol., **22(8)**, 862-871

Jacobs, L., Emerson, S. and Skei, J. (1985) Partitioning and transport of metals across the O_2/H_2S interface in a permanently anoxic basin: Framvaren Fjord, Norway. Geochim. Cosmochim. Acta., **49**, 1433-1444

Jahnke, R.A. (1988) A simple reliable and inexpensive pore-water sampler. Limnol. Oceanogr., **33**, 483-487

Johnson, K.S., Stout, P.M., Berelson, W.M., and Sakamoto-Arnold, C.M. (1988) Cobalt and Copper distributions in the waters of Santa Monica Basin, California. Nature, **332**, 527-530

Johnson, K.S., Berelson W.M., Coale, K.H., Coley, T.L., Elrod, V.A., Fairey, W.R., Iams, H.D., Kilgore, T.E. and Nowicki, J.L. (1992) Manganese flux from continental shelf margins in a transect through the oxygen minimum. Submitted

Katz, A. and Kaplan, I.R. (1981) Heavy metals behavior in coastal sediments of southern California: a critical review and synthesis. Marine Chemistry, **10**, 261-299.

Klinkhammer, G.P. (1980) Early digenesis in sediments from the eastern equatorial Pacific, II. Pore water metal results. Earth Planet. Sci. Lett., **49**, 81-101

Klinkhammer, G., Heggie, D.T. and Graham, D.W. (1982) Metal diagenesis in oxic marine sediments. Earth Planet. Sci. Lett., **61**, 211-219.

Klump, J., and Martens, C.S. (1989) The seasonality of nutrient regeneration in an organic-rich coastal sediment: Kinetic modeling of changing pore-water nutrient and sulfate distributions. Limnol. Oceanogr., **34(3)**, 559-577

Li, Y.H. and Gregory, S. (1974) Diffusion of ions in sea water and deep-sea sediments. Geochim. Cosmochim. Acta, **38**, 703-714.

Martin J.H., Bruland, K.W., and Broenkow, W.W. (1976) Cadmium transport in the California current. In: Marine Pollutant Transfer, H. Windom and R. Duce, editors, D.C. Heath, Lexington, Ma., 159-184

Morel F.M.M., Westfall, J.C., O'Melia, C.R., and Morgan J.J. (1975) Fate of trace metals in the Los Angeles County wastewater discharge. Environ. Sci. Technol., **9**, 756-761.

Paulson, A.J., Curl, Jr., H.C., and Cokelet, E.D. (1991) Remobilization of Cu from marine particulate matter and from sewage. Marine Chemistry, **33**, 41-60.

Robinson, R.A. and Stokes, R.H. (1959) Electrolyte Solutions Butterworth & Co. (publ.) Ltd

Saager, P.M., Sweerts, J-P., and Ellermeijer, H.J. (1990) A simple pore water sampler for coarse sandy sediments of low porosity. Limnol. Oceanogr., **35(3)**, 747-751

Sakamoto-Arnold, C.M. and Johnson, K.S. (1987) Determination of picomolar levels of cobalt in seawater by flow injection analysis with chemiluminescence detection. Analyt. Chem., **59**, 1789-1794

Sawlan, J.J. and Murray, J.W. (1983) Trace metal remobilization in the interstitial waters of red clay and hemipelagic marine sediments. Earth Planet. Sci. Lett., **64**, 213-230.

Shaw, T.J., Gieskes, J.W., and Jahnke, R.A. (1990) Early diagenesis in differing depositional environments: The response of transition metals in pore water. Geochim. Cosmochim. Acta, **54**, 1233-1246.

Southern California Coastal Water Research Project (1986-1989)

Strickland, J. and Parsons, T. (1972) A Practical Handbook for Seawater Analysis, Ottawa, Canada, Canadian Fisheries Research Board.

Sweeney, R.E. and Kaplan, I.R. (1980) Tracing flocculent industrial and domestic sewage transport on San Pedro shelf, Southern California, by nitrogen and sulphur isotope ratios. Marine Environ. Research, 3, 215-224

Sweeny, R.E., Kalil, E.K., and Kaplan, I.R. (1980) Characterization of domestic and industrial sewage in Southern California coastal marine sediments using nitrogen, sulfur and uranium tracers. Marine Environ. Research, **3**, 225-243

Wilson, T.R.S., Thomson, J., Hydes, D.J., Colley, S., Culkin, F. and Sorenson, J. (1986) Oxidation Fronts in Pelagic Sediments: Diagenetic Formation of Metal-Rich Layers. Science, **232**, 972-974

CHAPTER 4

Conclusions

The region of sediment near the sediment-water interface is a dynamic and complex zone of chemical and biological activity. The purpose of this study was to develop methods which would accurately sample the pore waters of this region and provide new data on the early diagenetic fate of trace metals. The modified whole core squeezing technique which has evolved through the course of this study has proven to be an effective, reliable and rapid method for the extraction of pore waters from sediments. Its use in addressing trace metal geochemistry has produced unique data over a wide range of physical and environmental conditions. The interpretation of this data is providing valuable clues to the understanding of trace metal cycling between sediments and the water column. Continued use of this technique is recommended for the study of trace metals in open ocean, nearshore and polluted sediments. Modifications of this technique may extend its usefulness to the study of other inorganic and organic compounds in sediments as well. The use of this technique, in determining chemical fluxes from the near interface region, should prove extremely valuable to the study of toxins and pollutants in marine and freshwater sediments. The work and data presented in this thesis should provide a strong foundation for continued research in this field.

APPENDIX

Bottom Depth-99m

Subcore I Station 17
35 35.39 N 121 14.78 W

Sample ID	Vol(ml)	Vol(mm)	Z(mm)	O2(%S)	O2(uM)	pH(mV)	pH	NH3(nM)	Mn(nM)	Fe(nM)	Co(pM)	Cu(nM)
1										50		
2				72	134					4		12
3									60	0	2935	
4										5		7
5	7.417	1.192								37		
6	7.58	1.218				-66	7.29	0.33	19	0	3417	7
7	7.436	1.195	0.00	71	132					40		
8	7.364	1.184	-1.79	67	125	-64	7.26	0.57		59		9
9	7.42	1.193	-3.67	65	121				113	110	8006	14
10	7.368	1.184	-5.58	56	105	-61	7.21	1.05		51		9
11	7.429	1.194	-7.57	50	94					142		8
12	7.46	1.199	-9.62	36	67	-55	7.1	2.72	234	346	10105	20
13	7.575	1.218	-11.75	27	50				274	435	10153	11
14	7.522	1.209	-13.90	20	37	-46	6.94	3.2	210	290	9877	5
15	7.644	1.229	-16.13	13	24				218	292	9718	3
16	7.3	1.173	-18.29	10	19	-51	7.03	3.68	207		9176	12
17	7.345	1.181	-20.49						214		9104	23
18	7.499	1.205	-22.75			-53	7.07	4.16	249		8502	11
19	7.289	1.172	-24.97							145		
20	7.466	1.200	-27.26	5	9	-52	7.05	5.59				
21	7.458	1.199	-29.56						277		9893	6
22	7.367	1.184	-31.84			-52	7.05	7.03		25		

Porosity	Flux(mM)	Flux(mM)	Flux(uM)	Flux(uM)	Flux(nM)	Flux(uM)
60%	-0.187	0.013	0.243	0.318	13.281	0.020
100%	-0.812	0.036	1.042	1.364	56.894	0.087

Bottom Depth- 100m

Subcore E Station 11
36 44.11 N 121 55.89 W

Sample ID	Vol(ml)	Vol(mm)	Z(mm)	O2(%S)	O2(uM)	pH(mV)	pH	NH3(nM)	Mn(nM)	Fe(nM)	Co(pM)	Cu(nM)	DOC(uM)
1									12.75	425	510	0	
2				52	128		6.98		54.1		1271	846	
3	7.292	1.172		26	65	-18			112.88	43	1371	51	166.05
4	7.274	1.169	0.00	23	56				156.67	52	1628	23	
5	6.992	1.124	-1.73	21	52		6.88		205.01	50	1850	38	189.28
6	7.104	1.142	-3.54	14	34	-10	6.8		336.65	654	2695	176	172.63
7	7.078	1.138	-5.41	9.7	24				468.7	3568	4358	405	236.98
8	6.685	1.075	-7.22	8.1	20	-5	6.72		493.51	5914	3722	697	213.95
9	6.995	1.124	-9.16	5	12.4				339.09	2289	2909	393	227.86
10	7.206	1.158	-11.22	3.6	8.9		6.75		320.31	1989	2150	349	
11	7.043	1.132	-13.26							1551		256	173.9
12	7.287	1.171	-15.41	2.5	6.2	-10				1360		226	
13	6.971	1.121	-17.51						321.96	866	1676	177	180.34
14	7.227	1.162	-19.70	1.8	4.5		6.79					130	
15	6.721	1.080	-21.77							449		114	186.24
16	7.283	1.171	-24.02						363.32	373	1828	61	
17	7.356	1.182	-26.32				6.82					61	
18	7.343	1.180	-28.63			-39			358	248		52	211.51
19	7.367	1.184	-30.95	0.2	0.67				452.09		2243	67	
20	7.148	1.149	-33.22						400	222		48	
21	7.27	1.169	-35.53						414				
22	6.59	1.059	-37.63						547.57		3409		415.55

Porosity	Flux(mM)	Flux(uM)	Flux(uM)	Flux(nM)	Flux(uM)	Flux(mM)
63%	-0.322	0.604	7.605	5.905	0.826	0.058
100%	-1.291	2.416	30.436	23.632	3.307	0.234

Bottom Depth-107m

Subcore A Station 1
36 13.91 N 121 52.60 W

Sample ID	Vol(ml)	Vol(mm)	Z(mm)	O2(%S)	O2(uM)	pH(mV)	pH	NH3(nM)	Mn(nM)	Fe(nM)	Co(pM)	Cu(nM)
1											16400	68
2	7.225	1.161		79	181			5.3			10100	26
3	7.671	1.233	0.00	57	132						25800	219
4	6.601	1.061	-1.44	33	75		6.99	2.1			20800	61
5	7.644	1.229	-3.14	23	53		6.88				27900	55
6	7.416	1.192	-4.82				6.88	4.8			25200	46
7	6.756	1.086	-6.39	21	48						23900	26
8	7.178	1.154	-8.09					12.2			32700	52
9	7.124	1.145	-9.80	15	35						33500	21
10	6.634	1.066	-11.41					15.3			42000	22
11	7.514	1.208	-13.26									
12	6.709	1.078	-14.93					18.8				
13	6.227	1.001	-16.49	14	33		6.48					
14	5.376	0.864	-17.85					24.3				
15	6.113	0.983	-19.40				6.76					
16	5.339	0.858	-20.76	11	26		6.76	27.5				
17	4.746	0.763	-21.98									
18	5.46	0.878	-23.38	9	20			30.6				
19	5.758	0.926	-24.87									
20	6.863	1.103	-26.64	4	9			32.7			50600	

Porosity	Flux(mM)	Flux(uM)	Flux(uM)	Flux(nM)	Flux(uM)
69%	-0.670			43.911	0.058
100%	-1.408			92.231	0.122

Bottom Depth-93m

Subcore H Station 17
35 35.78 N 121 14.10 W

Sample ID	Vol(ml)	Vol(mm)	Z(mm)	O2(%S)	O2(uM)	pH(mV)	pH	NH3(nM)	Mn(nM)	Fe(nM)	Co(pM)	Cu(nM)
1										353	500	316
2										74	638	43
3	6.507	0	0.00							379	2220	63
4	7.01	1.127	-1.56							302	1840	37
5	7.06	1.135	-3.18							277	3080	29
6	6.773	1.089	-4.76							125	2930	22
7	6.34	1.019	-6.27							94	3180	14
8	6.47	1.040	-7.84							115	2110	16
9	6.453	1.037	-9.43							128	2940	16
10	7.635	1.227	-11.34							141	3650	22
11	7.125	1.145	-13.15							133	4390	28
12	7.259	1.167	-15.01									
13	7.086	1.139	-16.85								3660	19
14	7.321	1.177	-18.77							116		
15	7.216	1.160	-20.67								3910	23
16	7.005	1.126	-22.52									
17	7.605	1.222	-24.55								3730	25
18	7.558	1.215	-26.58									
19	6.985	1.123	-28.45							121	4170	26
20	7.22	1.161	-30.40									
21	6.74	1.083	-32.22									
22	7.286	1.171	-34.19							125	3620	40

Porosity	Flux(uM)	Flux(uM)	Flux(nM)	Flux(uM)
69%		-0.706	1.973	-0.114
100%		-1.572	4.394	-0.254

Bottom Depth- 235m

Subcore C Station 6
35.23.39 N 121 04.59 W

Sample ID	Vol(ml)	Vol(mm)	Z(mm)	O2(%S)	O2(uM)	pH(mV)	pH	NH3(nM)	Mn(nM)	Fe(nM)	Co(pM)	Cu(nM)
1										579	1267	571
2				30	75	-49	7.06	2	31	35	376	1.7
3	7.52	1.209	0.00	20	50	-50	7.08		[illegible]	23	144	2.6
4	7.557	1.215	-1.50			-47	7.02	2	16?	6	509	0.2
5	7.633	1.227	-3.04	14	36	-45	6.99		34	102	306	1.6
6	7.582	1.219	-4.60			-41	6.91	2.8	81	251	940	36
7	6.862	1.103	-6.03	5.6	14	-42	6.93		107	840	1110	70
8	7.327	1.178	-7.58	3.7	9			5.2	119	976	1036	187
9	7.527	1.210	-9.19	2.6	6.6	-43	6.95		120	1474	884	237
10	6.517	1.048	-10.59					7.2	127	1803	1185	287
11	6.951	1.117	-12.11	0.8	2					1380	797	
12	6.01	0.966	-13.43					9	126	996		164
13	6.441	1.035	-14.85			-45	6.98			613	903	
14	7.101	1.141	-16.43					11		577		
15	7.176	1.153	-18.04	0	0	-44	6.97			671		14
16	7.369	1.185	-19.69					14		565	1775	
17	7.287	1.171	-21.33							479		4
18	7.337	1.179	-23.00					19		449		
19	7.192	1.156	-24.63							351	940	
20	7.402	1.190	-26.32					23		342		
21	7.248	1.165	-27.97							278		
22	7.099	1.141	-29.59			-47	7.02	25.9	210	252	1114	
23	7.501	1.206	-31.31							233		4
24	7.273	1.169	-32.98									
25	7.017	1.128	-34.59			-49	7.06				953	

Porosity	Flux(mM)	Flux(uM)	Flux(uM)	Flux(nM)	Flux(uM)
77%	-0.379	0.180	0.866	3.025	0.127
100%	-1.054	0.382	1.835	6.407	0.269

Bottom Depth-519m

Subcore B Station 5
35 39.26 N 121 27.67 W

Sample ID	Vol(ml)	Vol(mm)	Z(mm)	O2(%S)	O2(uM)	pH(mV)	pH	NH3(nM)	Mn(nM)	Fe(nM)	Co(pM)	Cu(nM)	DOC(uM)
1											1250	21	
2								-1			910	32	
3	6.932	1.114				-66	7.36		19		1140	11	
4	7.272	1.169						0	29		1010	29	
5	7.305	1.174		29	76				93		1610	67	153.74
6	7.43	1.194	0.00	26	68	-62	7.28	0	188		2080	33	436.61
7	6.611	1.063	-1.24			-53	7.13		90		1900	46	165.92
8	7.498	1.205	-2.67			-55	7.16	1.7	384		1660	142	163.77
9	6.918	1.112	-4.00	17	44				71		1840	22	142.27
10	7.322	1.177	-5.43			-43	6.95	4.5	82		2020	10	477.76
11	6.432	1.034	-6.70	13	34	-40	6.89						638.13
12	6.751	1.085	-8.05			-39	6.88	8.3	93		1580		211.8
13	6.452	1.037	-9.35	11	28	-38	6.86						
14	7.105	1.142	-10.79					14	89		1990		250.51
15	6.428	1.033	-12.10	7	18								
16	7.448	1.197	-13.63			-37	6.84	14	108		1620		230.7
17	6.667	1.072	-15.01	5	12								
18	7.033	1.131	-16.47					17					412.53
19	7.353	1.182	-18.01	3	7.2	-36	6.82		124		1560		
20	7.408	1.191	-19.56					21					
21	6.752	1.085	-20.98	1	4								
22	7.215	1.160	-22.50			-36	6.82	23	152		1330		327.22

Porosity	Flux(mM)	Flux(uM)	Flux(uM)	Flux(nM)	Flux(uM)	Flux(uM)
81%	-0.422	-0.035		-0.214	-0.082	-0.016
100%	-0.761	-0.064		-0.388	-0.149	-0.028

Bottom Depth-642m

Subcore L Station 7
35 12.34 N 121 18.42 W

Sample ID	Vol(ml)	Vol(mm)	Z(mm)	O2(%S)	O2(uM)	pH(mV)	pH	NH3(nM)	Mn(nM)	Fe(nM)	Co(pM)	Cu(nM)
1												
2				44	127	-53	7.07	0.82	22		0	11
3	6.717	1.080										
4	7.467	1.200						0.82	16		436	6
5	6.7	1.077										
6	7.516	1.208		42	120	-53	7.07	0.82	13		676	4.6
7	6.73	1.082	0.00	42	120	-53	7.07					
8	7.509	1.207	-1.34					1.06	14		122	4.4
9	6.768	1.088	-2.56	40	114							
10	7.525	1.210	-3.93	38	107	-53	7.07	1.29	15		234	6
11	7.335	1.179	-5.28	35	99	-50	7.02		20		240	4.4
12	7.402	1.190	-6.66	26	74	-44	6.91	1.29	30		96	3.6
13	7.544	1.213	-8.08	132	36	-33	6.72		46		778	27
14	7.4	1.189	-9.48	5	14	-42	6.88	1.29	38		95	15
15	7.454	1.198	-10.91	0.1	0.4				40		113	8
16	7.362	1.183	-12.32					2.23	43		511	8
17	7.284	1.171	-13.73			-41	6.86		55		0	5.4
18	7.397	1.189	-15.16	0.2	0.8			3.64				
19	7.32	1.177	-16.59	0	0				56		110	17
20	7.07	1.136	-17.97			-42	6.88	5.75				
21	6.596	1.060	-19.27									
22	7.231	1.162	-20.69					7.63	72		373	202

Porosity	Flux(mM)	Flux(uM)	Flux(uM)	Flux(uM)	Flux(uM)
86%	-0.315	0.022		0.487	0.000
100%	-0.480	0.034		0.742	0.000

Bottom Depth-650m

Subcore G Station 7
35 11.94 N 121 18.14 W

Sample ID	Vol(ml)	Vol(mm)	Z(mm)	O2(%S)	O2(uM)	pH(mV)	pH	NH3(nM)	Mn(nM)	Fe(nM)	Co(pM)	Cu(nM)	DOC(uM)
1									9	69	527		
2				74	210			0.24	12	73	587	12	
3	7.443	1.196							12	28	805		145.62
4	7.584	1.219				-63	7.24	0.72	12	58	725	11.4	
5	7.592	1.220	0.00	60	172.7				17	86	879		141.53
6	7.264	1.168	-1.32	57	162.2			0.72	39	103	664	7.5	121.09
7	7.165	1.152	-2.64	54	154.4	-58	7.16		21	213	887		134.83
8	7.552	1.214	-4.05	45	130.4			0.96	56	491	1673	15.4	104.83
9	7.331	1.178	-5.43	24	69.3				36	654	724		144.6
10	7.581	1.219	-6.88	16	44.9			0.48	27	64	177	8.4	125.06
11	7.012	1.127	-8.23	10	29.1	-48	6.98		22	85	1025		
12	7.278	1.170	-9.64	8	21.9			0	27	124	363	0.8	139.2
13	7.443	1.196	-11.10	5	14.8				17	150	1717		
14	7.358	1.183	-12.55	4.5	12.8	-47	6.96	0.72	28	186	836	7.5	149.54
15	7.331	1.178	-14.00						26	273			
16	7.339	1.180	-15.47					1.68				9.9	202.21
17	6.784	1.090	-16.82						28	119	1031		
18	7.052	1.134	-18.24	4.3	12.2	-47	6.96	3.36				19.3	
19	7.144	1.148	-19.68						24	111	1042		342.26
20	6.936	1.115	-21.08					6				57.7	
21	6.873	1.105	-22.47	5.7	16.4	-47	6.96						
22	7.148	1.149	-23.92						37	84	1659	37.3	381.77

Porosity	Flux(mM)	Flux(uM)	Flux(uM)	Flux(nM)	Flux(uM)	Flux(mM)
84%	-1.209	0.065	2.173	-0.593	0.003	-0.072
100%	-2.039	0.092	3.08	-0.84	0.005	-0.102

Bottom Depth-1010m

Subcore K Station 12
35 27.83 N 121 36.33 W

Sample ID	Vol(ml)	Vol(mm)	Z(mm)	O2(%S)	O2(uM)	pH(mV)	pH	NH3(nM)	Mn(nM)	Fe(nM)	Co(pM)	Cu(nM)	DOC(uM)
1													
2								0	21	5	915	11	
3	6.783	1.090											
4	7.364	1.184		23	60			0	3	0	853	9	
5	6.645	1.068				-62	7.22						
6	7.433	1.195						0	15	0	775	17	161
7	6.77	1.088											
8	7.379	1.186	0.00	15.6	41	-59	7.17	0	19	43	875	15	152
9	6.776	1.089	-1.23	14.8	38.8								121.63
10	7.478	1.202	-2.61					0	16	46	914	13	212.32
11	7.462	1.199	-4.00	12.8	33.8				21		919	39	175.76
12	7.365	1.184	-5.39	12	31.4	-58	7.15	0.24	26	208	926	22	174.35
13	7.461	1.199	-6.81	7.3	19.4	-50	7.02		39	1984	1090	91	212.32
14	7.303	1.174	-8.22	5.8	15.3	-46	6.95	4.08	171	5397	2002	475	212.32
15	7.397	1.189	-9.66	2.5	6.7	-50	7.02		51	1559	968	82	216.89
16	7.512	1.207	-11.13			-52	7.05	2.16	50	131	588	10	
17	7.527	1.210	-12.61	0.3	0.7				62	43	531	4.2	175.06
18	7.288	1.171	-14.05			-52	7.05	2.64	62	23			
19	7.383	1.187	-15.53						61	23	568		197.55
20	7.404	1.190	-17.01					3.36				0	
21	6.732	1.082	-18.36										
22	6.465	1.039	-19.66						64	9	335		330.15
23	6.847	1.101	-21.05			-52	7.05					3.8	

Porosity	Flux(mM)	Flux(uM)	Flux(uM)	Flux(nM)	Flux(uM)	Flux(mM)
84%	-0.135	0.024	0.636	0.197	0.027	0.033
100%	-0.220	0.039	1.040	0.321	0.044	0.054

Bottom Depth-1042m

Subcore F Station 12
35 27.03 N 121 36.51 W

Sample ID	Vol(ml)	Vol(mm)	Z(mm)	O2(%S)	O2(uM)	pH(mV)	pH	NH3(nM)	Mn(nM)	Fe(nM)	Co(pM)	Cu(nM)
1									19	62		155
2						-77	7.49	0	9	66	0	69
3	7.689	1.236							6	25	1.12	51
4	7.76	1.247				-74	7.43	0	11	24	151	37
5	7.481	1.203							1	28	78.6	34
6	7.389	1.188						0	6	50	84.4	13
7	7.506	1.207	0.00	83	217				10	71	63	16
8	7.426	1.194	-1.32					0	8	43	612	15
9	7.645	1.229	-2.70	76	200.3	-69	7.35			64	101	11
10	7.745	1.245	-4.11	66	172.8			0	21	136	239	16
11	7.662	1.232	-5.53	57	149.3				35	296	137	23
12	7.621	1.225	-6.95	45	116.7	-62	7.23	0.24	37	414	1038	31
13	7.62	1.225	-8.39	26	69.4	-56	7.12		178	2576	1118	108
14	7.772	1.249	-9.86	20	51.5	-50	7.02	4.08	732	6324	1568	260
15	7.53	1.210	-11.30	17	45.9	-59	7.17		118	3371	996	116
16	7.688	1.236	-12.78	17	43.9	-60	7.19	2.16	82	1350	131	36
17	6.708	1.078	-14.08	13	33.2							
18	7.576	1.218	-15.55	12	31.5			2.64	61	558	0	13
19	6.933	1.114	-16.91	12	31.2	-58	7.16					
20	7.596	1.221	-18.39	11	27.8			3.36	72	234	1152	11
21	6.501	1.045	-19.67	10	25.1							
22	6.589	1.059	-20.97			-58	7.16					

Porosity	Flux(mM)	Flux(uM)	Flux(uM)	Flux(nM)	Flux(uM)
86%	-0.970	0.088	0.887	0.292	0.028
100%	-1.311	0.119	1.199	0.394	0.037

Bottom Depth-2006m

Subcore M Station 10
35 12.61 N 121 53.85 W

Sample ID	Vol(ml)	Vol(mm)	Z(mm)	O2(%S)	O2(uM)	pH(mV)	pH	NH3(nM)	Mn(nM)	Fe(nM)	Co(pM)	Cu(nM)
1												
2				28	72	-54	7.09	1.53	12	24	1374	
3	7.292	1.172										11.6
4	7.489	1.204	0.00	25	63			2	83	36	1189	
5	7.492	1.204	-1.48	23	58				100	24	1055	
6	7.542	1.212	-3.01	16	40			2.7	127	71	1406	23
7	7.538	1.212	-4.56	7	18	-54	7.09		564	2434	2003	140
8	7.634	1.227	-6.15	2	6	-53	7.07	7.16	767	3471	2598	197
9	7.424	1.193	-7.72	1.4	3				877	4012	2953	245
10	7.472	1.201	-9.32			-52	7.05	9.03	890	4347	3033	253
11	7.482	1.203	-10.94						948	5494	3485	273
12	7.213	1.159	-12.51	0.5	1.4	-51	7.03	11.14				294
13	7.549	1.213	-14.17						1091	6723	3976	347
14	7.331	1.178	-15.80	0	0	-50	7.02	11.38				349
15	7.487	1.203	-17.47									459
16	7.452	1.198	-19.14					13.72	984	7933	4385	603

Porosity	Flux(mM)	Flux(uM)	Flux(uM)	Flux(nM)	Flux(uM)
77%	-0.486	0.229	0.203	1.260	0.066
100%	-1.020	0.480	0.427	2.646	0.139

Bottom Depth - 66m

POC - 3.87%
PON - 0.31%

Palos Verdes Station 1
33 42.1 N 118 20.7 W

Sample ID	Vol(ml)	Vol(mm)	Z(mm)	NH3(nM)	PO4(nM)	Cu(nM)	Mn(nM)	Fe(nM)	Co(pM)
1	20.19	3.245	2	39	3.5	950			
2	16.46	2.646	0	62	11.2	1336			
3	12.98	2.086	-2.34	93	19	1215			
4	9.34	1.501	-4.06	118	18.8	1061			
5	18.37	2.953	-7.50	139	19.8	1148			

Porosity	Flux(mM)	Flux(mM)	Flux(uM)	Flux(uM)	Flux(uM)	Flux(nM)
83%	1.310	0.218	2.300	0.000	0.000	0.000
100%	1.901	0.317	3.338	0.000	0.000	0.000

Bottom Depth - 66m

POC - 3.01%
PON - 0.20%

Palos Verdes Station 2
33 43.27 N 118 22.83 W

Sample ID	Vol(ml)	Vol(mm)	Z(mm)	NH3(nM)	PO4(nM)	Cu(nM)	Mn(nM)	Fe(nM)	Co(pM)
1	50.19	8.068	2	110	8.4	398			
2	18.76	3.016	0	125	10.2	910			
3	16.67	2.680	-3.00	159	16.2	2379			
4	17.55	2.821	-6.26	124		2213			
5	16.48	2.649	-9.39	192	22.9	1593			
6	18.81	3.024	-13.03	213	35.4	1411			
7	17.24	2.771	-16.42	215	27.3	1431			

Porosity	Flux(mM)	Flux(mM)	Flux(uM)	Flux(uM)	Flux(uM)	Flux(nM)
71%	0.818	0.096	7.264	0.000	0.000	0.000
100%	1.624	0.190	14.409	0.000	0.000	0.000

Bottom Depth - 64m

POC - 3.54%
PON - 0.16%

Palos Verdes Station 3
33 45.3 N 118 26.4 W

Sample ID	Vol(ml)	Vol(mm)	Z(mm)	NH3(nM)	PO4(nM)	Cu(nM)	Mn(nM)	Fe(nM)	Co(pM)
1	38.14	6.131	2	6.5	2.2	65			
2	18.71	3.007	0	5.1	2.1	324			
3	19	3.054	-3.42	8.2	2.8	986			
4	17.5	2.813	-6.68	13.6	3.5	759			
5	19.77	3.178	-10.45	17.7	4.3	156			
6	19.97	3.210	-14.34	23.1	3.9	379			
7	16.79	2.699	-17.65	31.7	4.3	1385			

Porosity	Flux(mM)	Flux(mM)	Flux(uM)	Flux(uM)	Flux(uM)	Flux(nM)
75%	0.073	0.011	3.205	0.000	0.000	0.000
100%	0.130	0.019	5.697	0.000	0.000	0.000

Bottom Depth -77m

Palos Verdes Station 4
33 44.31 N 118 25.23 W

Sample ID	Vol(ml)	Vol(mm)	Z(mm)	O2(%S)	O2(uM)	pH(mV)	pH	NH3(nM)	Mn(nM)	Fe(nM)	Co(pM)	Cu(nM)
1				34	81.6						1064	66
2			2	29	69.6	-4	7.40		246			
3	7.424	1.193	0	15	36	-7	7.45		247		765	54
4	7.527	1.210	-1.49	13	31.2	-9.9	7.50		242		1377	27
5	7.392	1.188	-2.98	11	26.4	15	7.07		335		1523	326
6	7.387	1.187	-4.50	4	9.6	26	6.88		1112		2694	1370
7	7.535	1.211	-6.07	0	0	-7.8	7.46		433		1892	596
8	7.422	1.193	-7.64			-14	7.57		490		1335	460
9	7.382	1.187	-9.22			-14.5	7.58		474		1232	496
10	7.441	1.196	-10.83			-15.1	7.59					
11	7.412	1.191	-12.45			-14.7	7.58		512		2137	513
12	7.394	1.189	-14.07			-17	7.62					
13	7.389	1.188	-15.71			-20.8	7.69		525		1844	866
14	7.382	1.187	-17.36			-21.9	7.71					
15	7.262	1.167	-18.99						534		2028	950
16	7.365	1.184	-20.64									
17	7.382	1.187	-22.31			-29	7.83		514		2105	1308
18	7.446	1.197	-24.00									
19	7.391	1.188	-25.68						523		2138	1268
20	7.457	1.199	-27.39			-33	7.90					
21	7.385	1.187	-29.07									
22	7.454	1.198	-30.78			-34	7.91		475		2062	1795
23	7.37	1.185	-32.47									
24	7.446	1.197	-34.18									
25	7.436	1.195	-35.89			-34	7.91		478		2332	1844

Porosity	Flux(mM)	Flux(mM)	Flux(uM)	Flux(uM)	Flux(nM)	Flux(uM)
74%	-0.344	0.000	2.773	0.000	6.914	4.717
100%	-0.628	0.000	5.064	0.000	12.625	8.613

Bottom Depth - 65m

Palos Verdes Station 5
33 43.31 N 118 22.94 W

Sample ID	Vol(ml)	Vol(mm)	Z(mm)	O2(%S)	O2(uM)	pH(mV)	pH	NH3(nM)	Mn(nM)	Fe(nM)	Co(pM)	Cu(nM)
1				49	117.6	-34	7.11					
2			2	40	96	-33.7	7.11		266		3724	142
3	7.456	1.198	0	27	64.8				311		3353	298
4	7.388	1.188	-1.49	18	43.2	-31.2	7.06		336		3961	278
5	7.396	1.189	-3.01	16	38.4	-29.3	7.03		380		4812	845
6	7.436	1.195	-4.57	8	19.2	-27.5	7.00		439		6529	2248
7	7.354	1.182	-6.14	3	7.2	-33.2	7.10		492		5246	4599
8	7.428	1.194	-7.74	0	0				528		4197	5066
9	7.417	1.192	-9.36			-33.3	7.10		579		3974	5143
10	7.478	1.202	-11.01									
11	7.445	1.197	-12.68			-35.3	7.14		583		3652	5747
12	7.609	1.223	-14.39									
13	7.417	1.192	-16.07			-38	7.18		644		3371	5897
14	7.492	1.204	-17.79									
15	7.31	1.175	-19.47						660		3175	
16	7.445	1.197	-21.18									
17	7.518	1.208	-22.93			-38	7.18		663		2685	6642
18	7.414	1.192	-24.65									
19	7.361	1.183	-26.37						630		2553	7405
20	7.376	1.186	-28.09			-42	7.25					
21	7.464	1.200	-29.84									
22	7.411	1.191	-31.58						623		2186	7250
23	7.419	1.193	-33.33									
24	7.421	1.193	-35.07									
25	7.427	1.194	-36.82			-40	7.22		640		2479	8065

Porosity	Flux(mM)	Flux(mM)	Flux(uM)	Flux(uM)	Flux(nM)	Flux(uM)
72%	-0.521	0.000	0.403	0.000	10.614	10.707
100%	-1.006	0.000	0.777	0.000	20.475	20.654

Bottom Depth- 66m

Palos Verdes Station 6
33 42.1 N 118 20.7 W

Sample ID	Vol(ml)	Vol(mm)	Z(mm)	O2(%S)	O2(uM)	pH(mV)	pH	NH3(nM)	Mn(nM)	Fe(nM)	Co(pM)	Cu(nM)
1												
2						-53	7.44		26		2187	6
3												
4	7.482	1.203	2	41	98.4	-48.7	7.36		96		1289	80
5	7.466	1.200	0	40	96	-45.7	7.31					
6	7.251	1.166	-1.31	25	60	-41	7.23		159		1264	401
7	7.403	1.190	-2.66	13	31.2	-39	7.20		168		2027	850
8	7.372	1.185	-4.02	10	24	-36	7.15		203		1905	
9	7.302	1.174	-5.39	5	12	-33	7.10		245		2754	1356
10	7.473	1.201	-6.80	3	7.2	-31	7.06		217		2404	2749
11	7.421	1.193	-8.22	2	4.8	-30.8	7.06		245		1999	4866
12	7.435	1.195	-9.65			-27.7	7.00		241		2398	3450
13	7.482	1.203	-11.10	0	0	-28.5	7.02		242		2132	3007
14	7.407	1.191	-12.54			-29.6	7.04		215		2262	6483
15	7.36	1.183	-13.99									
16	7.365	1.184	-15.44			-29.2	7.03		249		1877	6436
17	7.323	1.177	-16.89									
18	7.499	1.205	-18.38									
19	7.368	1.184	-19.85			-27.3	7.00		313		1785	5972
20	7.435	1.195	-21.34									
21	7.339	1.180	-22.81									
22	7.537	1.212	-24.33			-25.3	6.96		317		2130	8034
23	7.375	1.185	-25.81									
24	7.41	1.191	-27.31									
25	7.471	1.201	-28.82			-24.8	6.96		242		1998	9830

Porosity	Flux(mM)	Flux(mM)	Flux(uM)	Flux(uM)	Flux(nM)	Flux(uM)
84%	-1.178	0.000	0.514	0.000	5.652	4.923
100%	-1.670	0.000	0.729	0.000	8.010	6.977